



17 **Abstract**

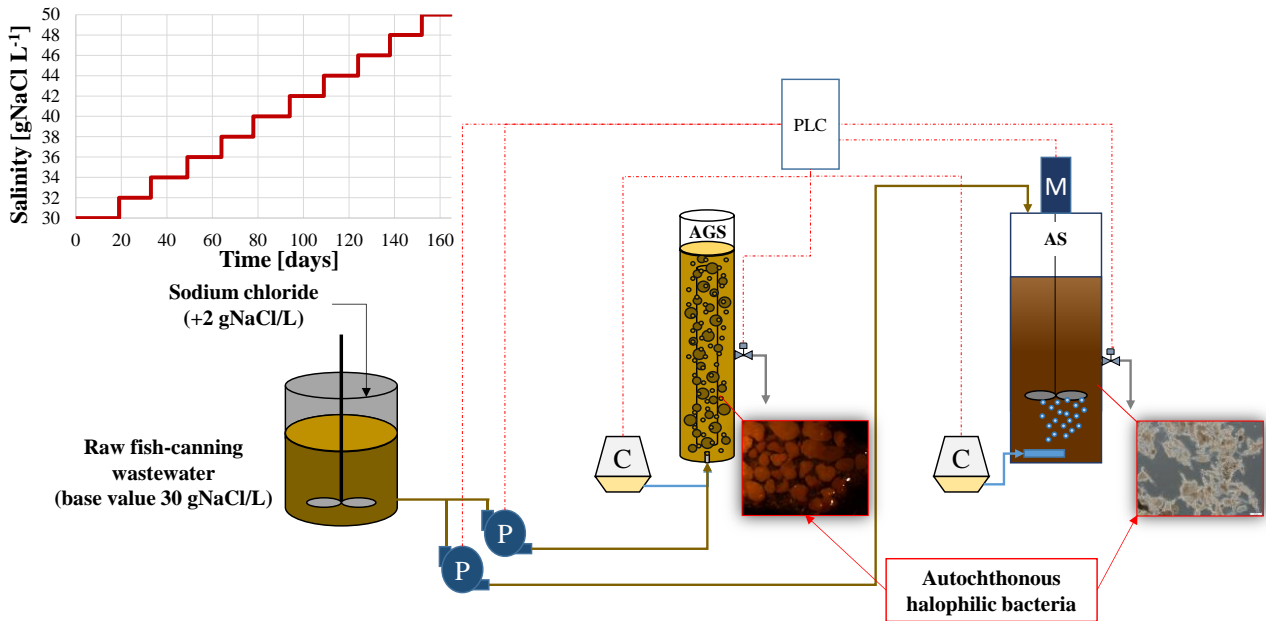
18 Biological nutrient removal performances and kinetics of autochthonous marine biomass in forms  
19 of activated sludge and aerobic granular sludge were investigated under different salinity and sludge  
20 retention time (SRT). Both the biomasses, cultivated from a fish-canning wastewater, were  
21 subjected to stepwise increases in salinity (+2 gNaCl L<sup>-1</sup>), from 30 gNaCl L<sup>-1</sup> up to 50 gNaCl L<sup>-1</sup>  
22 with the aim to evaluate the maximum potential in withstanding salinity by the autochthonous  
23 marine biomass. Microbial marine species belonging to the genus of Cryomorphaceae and of  
24 Rhodobacteraceae were found dominant in both the systems at the maximum salinity tested (50  
25 gNaCl L<sup>-1</sup>). The organic carbon was removed with a yield of approximately 98%, irrespective of the  
26 salinity. Similarly, nitrogen removal occurred via nitrification-denitrification and was not affected by  
27 salinity. The ammonium utilization rate and the nitrite utilization rate were approximately of 3.60  
28 mgNH<sub>4</sub>-N gVSS<sup>-1</sup>h<sup>-1</sup> and 10.0 mgNO<sub>2</sub>-N gVSS<sup>-1</sup>h<sup>-1</sup>, respectively, indicating a high activity of  
29 nitrifying and denitrifying bacteria. The granulation process did not provide significant  
30 improvements in the nutrients removal process likely due to the stepwise salinity increase strategy.  
31 Biomass activity and performances resulted affected by long SRT (27 days) due to salt  
32 accumulation within the activated sludge flocs and granules. In contrast, a lower SRT (14 days)  
33 favoured the discharge of the granules and flocs with higher inert content, thereby enhancing the  
34 biomass renewing.

35 The obtained results demonstrated that the use of autochthonous-halophilic bacteria represents a  
36 valuable solution for the treatment of high-strength carbon and nitrogen saline wastewater in a wide  
37 range of salinity. Besides, the stepwise increase in salinity and the operation at low SRT enabled  
38 high metabolic activity and to avoid excessive accumulation of salt within the biomass aggregates,  
39 limiting their physical destructuration due to the increase in loosely-bound exopolymers.

40

41 **Keywords:** Activated sludge; aerobic granular sludge; autochthonous-halophilic bacteria; shortcut  
42 nitrification; saline wastewater.

43 **Graphical abstract**



44

45

46 **Research Highlights**

- 47 • Autochthonous marine bacteria were cultivated as granular and activated sludge
- 48 • Biomass metabolic kinetics were evaluated at different salinity and SRT
- 49 • Salinity did not affect the biomass kinetics within the range of 30-50 gNaCl L<sup>-1</sup>
- 50 • Biomass activity and performances decreased for both system because of a long SRT
- 51 • Destructuration of the microbial bioaggragates occurred due to salt accumulation

52

53

## 54 **1. Introduction**

55 Nowadays, several activities, including petroleum, chemical and fish canning, produce large  
56 amount of wastewaters featured by high salt (chloride) concentration. In many cases, these  
57 wastewaters contain significant concentrations of biochemical oxygen demand (BOD), chemical  
58 oxygen demand (COD), total suspended solids (TSS) and total nitrogen (TN) (Chowdhury et al.,  
59 2010; Corsino et al., 2016).

60 Chemical and physical treatments, like membrane separation, ion exchange or electro dialysis have  
61 been widely investigated in the past (Fan et al., 2011; Muthukumaran and Baskaran, 2013).  
62 Although these methods are highly performing, they lead to secondary pollution (chemicals  
63 disposal) and are less cost-effective than biological treatments (energy and chemicals consumption);  
64 therefore they are currently limited only to specific applications (He et al., 2017).

65 Whereas biological treatments are widely recognized as cost-effective, their application in the field  
66 of industrial saline wastewater still represent a challenge. Indeed, one of the main drawbacks when  
67 treating saline wastewater is related to plasmolysis that involves the breaking of the cellular  
68 membrane, leading to the cell death (Lefebvre and Moletta, 2006). This phenomenon occurs when  
69 the solute concentration in the cytoplasm is higher than that in the surrounding environment.  
70 Similarly, plasmolysis could occur when the aqueous environment is hypertonic compared to the  
71 cytoplasm.

72 Although several studies demonstrated that the acclimation of activated sludge (AS) to salinity can  
73 be successfully achieved, the main bottleneck consists in the removal efficiencies of such salt-  
74 adapted systems (Campo et al., 2018; Lefebvre and Moletta, 2006; Zhang et al., 2017). To  
75 overcome this drawback, many authors suggested the use of aerobic granular sludge (AGS), since  
76 bacteria bio-aggregation could help to operate at higher salinity and faster kinetics as well (Wang et  
77 al., 2017; Wang et al., 2015). Nevertheless, the research findings suggested that halo-tolerant  
78 biomass, even in the form of granular sludge, totally lose its metabolic functionalities over a certain  
79 salinity level ( $> 20 \text{ g NaCl L}^{-1}$ ) (Jemli et al., 2015), thereby resulting in loss of removal efficiencies.

80 Recently, Chen et al. (Chen et al., 2018) demonstrated that microbial community diversity and  
81 richness, as well as removal performance for nitrogen and organic carbon deteriorated with  
82 increasing in salinity from 0 gNaCl L<sup>-1</sup> to 20 gNaCl L<sup>-1</sup>. The authors observed that salinity inhibited  
83 the dehydrogenase activity of activated sludge, thus decreasing bacterial metabolic activity. For  
84 these reasons, many researchers encouraged the use of halophilic bacteria for the biological  
85 treatment of high-strength saline wastewater (Gomes et al., 2018; Guo et al., 2016). Recently,  
86 several studies on the treatment of saline and hypersaline wastewater by means of halophilic  
87 biomass were carried out (Cui et al., 2016; Oren, 2010; Zhuang et al., 2010). Among these,  
88 Capodici et al. (2018) successfully cultivated autochthonous activated sludge from a real fish-  
89 canning wastewater. The authors assumed the presence of autochthonous active biomass in their  
90 study and speculated that it may be belonged to halophilic strains because of their ability to survive  
91 in hypersaline saline environment (>30 gNaCl L<sup>-1</sup>). The removal efficiencies BOD and TSS were  
92 higher than 90%. Similarly, more than 95% of the nitrogen was removed via shortcut nitrification-  
93 denitrification. Partial nitrification, or nitrification, naturally occurs treating saline wastewater  
94 because nitrite oxidizing bacteria (NOB) are more sensitive to the salt concentration than the  
95 ammonium oxidizing bacteria (AOB). However Capodici and coauthors tested the effectiveness of  
96 the autochthonous biomass only at 30 gNaCl L<sup>-1</sup> of salinity. Therefore, the ability of these bacteria  
97 to survive at higher salinity and its performances were not tested so far. Furthermore, it is possible  
98 to speculate that bio-aggregation of these bacteria in aerobic granular sludge (AGS), could represent  
99 a further advantage, thereby enhancing the biological performances or enabling the possibility to  
100 operate at higher salinity.

101 Another issue concerning the treatment of saline wastewater is related to the choice of a proper  
102 sludge retention time (SRT). Indeed, although at high salinity the biomass yield decreased, thereby  
103 limiting the sludge wasting (Ching and Redzwan, 2017), longer SRT could result in excessive  
104 "ageing" of the sludge because of accumulation of inert material within the flocs or granules. This  
105 in turn affects the biological performances because of the decrease in the biomass active fraction in

106 the system. Therefore, the choice of a proper SRT allow to avoid the decay of biological  
107 performances in the long term.

108 To the authors' knowledge, no studies reporting about the performances and the kinetics of  
109 autochthonous marine biomass at salinity higher than 30 gNaCl L<sup>-1</sup> nor the effects of SRT exist.  
110 Additionally, specific molecular analysis aimed at identifying these bacteria were not performed up  
111 to now. In this respect, identification of bacterial communities is indispensable for a better  
112 understanding of the biological processes that enable the nutrient removal, especially for the  
113 treatment of not conventional wastewater.

114 The purpose of this study was to validate the approach of cultivating autochthonous marine biomass  
115 for the treatment of saline wastewater and to test its maximum potentiality in terms of salinity  
116 withstanding. With this aim, this study investigated the biological nutrient removal efficiencies and  
117 the metabolic kinetics of autochthonous marine biomass derived from fish-canning wastewater, in  
118 forms of activated sludge and granular sludge, in a range of salinity between 30 gNaCl L<sup>-1</sup> and 50  
119 gNaCl L<sup>-1</sup> at different SRTs.

120

## 121 **2. Materials and Method**

### 122 *2.1 Reactors set-up*

123 Two sequencing batch reactors (SBR), one with aerobic granular sludge (AGS-SBR) and the other  
124 with flocculent activated sludge (AS-SBR) were operated. As reported in previous studies  
125 (Capodici et al., 2018; Corsino et al., 2018), because the biomass retention capacity of the AGS  
126 reactor was double than the AS, with the aim to compare the performances of those systems  
127 operating with the same biomass amount, the volume of the AS-SBR was chosen as the double of  
128 the AGS-SBR. More precisely, the AGS-SBR was a column-type (100 cm height) with a working  
129 volume of 4 L (internal diameter of 8.6 cm) and was characterized by an internal riser 50 cm high  
130 with an internal diameter of 5.4 cm. The AS-SBR had an operating volume of 8 L. Both the SBRs  
131 were equipped with a feeding pump and a solenoid valve for the effluent discharge placed at the

132 mid-point of the reactor yielding a volumetric exchange ratio (VER) equal to 50%. The volume of  
133 the raw wastewater treated per day was equal to 4 L and 8 L for the AGS-SBR and for the AS-SBR  
134 respectively. Therefore, the hydraulic retention time (HRT) was equal to 24 hours in both the  
135 reactors.

136 The AGS-SBR was operated on a 12 h cycle divided into 60 minutes of not-aerated influent upflow  
137 feeding, 10 h and 50 min of aeration (650 min), 5 min of settling and 5 min of effluent discharge.  
138 Air was introduced via a fine bubble aerator at the base of the reactor at a flow rate of 3 L min<sup>-1</sup> so  
139 that the superficial air velocity was approximately of 2.4 cm sec<sup>-1</sup>. The AS-SBR cycle included 60  
140 minutes of influent feeding (mixed and not-aerated), 9 h and 30 min (570 min) of aeration, 60 of  
141 anoxic mixing followed by 5 minutes of aeration to favour nitrogen stripping, 20 minutes of settling  
142 and 5 minutes of effluent discharge. The length of aerated/not-aerated period was set in order to  
143 maximize nitrogen removal efficiency. A stirrer device provided the mixing during the non-aerated  
144 period and a fine bubble diffuser provided the air supply. A Programmable Logic Controller (PLC)  
145 automatically handled the SBRs cycling operations.

146 The dissolved oxygen (DO) concentration within the bulk was maintained close to the saturation  
147 value according to the temperature and salinity.

148

## 149 *2.2 Experimental set-up*

150 The AGS-SBR and the AS-SBR were monitored for 165 days. Both the reactors were seeded with  
151 autochthonous activated sludge derived from a fish-canning wastewater. For the cultivation of this  
152 sludge, a parent reactor working as a conventional SBR was started-up without an activated sludge  
153 inoculum. More precisely, this reactor was filled with raw fish-canning wastewater and was  
154 operated with a complete sludge retention strategy until the autochthonous activated sludge  
155 developed. For further details on the cultivation of the autochthonous biomass, the reader is referred  
156 to the literature (Capodici et al., 2018).

157 The fish-canning wastewater was collected from a local industry that produces canned anchovies  
 158 (Palermo, Italy). The raw fish-canning wastewater was collected from the canning section of the  
 159 industry, where the wastewater had a salt concentration of approximately 150 g NaCl L<sup>-1</sup>. Then, the  
 160 raw fish-canning wastewater was diluted with tap water 1:5 (v/v) to obtain a salt concentration  
 161 approximately equal to that of the wastewater at the outlet of the industry (30 g NaCl L<sup>-1</sup>). After  
 162 dilution, the COD and the BOD<sub>5</sub> concentration resulted on average in approximately 800 mg L<sup>-1</sup>  
 163 respectively, whereas the TN and the NH<sub>4</sub>-N were on average equal to 150 mg L<sup>-1</sup> and 115 mg L<sup>-1</sup>,  
 164 respectively (Table 1).

165 The AGS-SBR and the AS-SBR were seeded with the autochthonous activated sludge derived from  
 166 the parent SBR reactor with a TSS concentration of approximately 3 gTSS L<sup>-1</sup>. Subsequently, both  
 167 the reactors were operated for approximately 3 months until steady conditions were achieved. The  
 168 salinity was kept constant to 30 gNaCl L<sup>-1</sup> until full granulation and stable performance (data not  
 169 discussed) were achieved in the AGS-SBR and AS-SBR systems. At the end of the start-up phase  
 170 (beginning of this study) the TSS concentration was of approximately 6.3 gTSS L<sup>-1</sup> and 13.1 gTSS  
 171 L<sup>-1</sup> in the AS and AGS reactor, respectively.

172

173 **Tab. 1:** Operating conditions for AGS-SBR and AS-SBR during the experimental phases.

	Phases										
	1	2	3	4	5	6	7	8	9	10	11
Duration [days]	15	15	15	15	15	15	15	15	15	15	15
Salinity [gNaCl L <sup>-1</sup> ]	30	32	34	36	38	40	42	44	46	48	50
COD [mg L <sup>-1</sup> ]	2035 (±206)	1989 (±131)	2164 (±147)	1921 (±151)	1857 (±97)	2104 (±86)	2373 (±106)	2098 (±141)	2238 (±153)	2127 (±134)	2094 (±191)
BOD <sub>5</sub> [mg L <sup>-1</sup> ]	865 (±136)	862 (±97)	843 (±62)	807 (±31)	727 (±44)	793 (±101)	760 (±59)	988 (±37)	897 (±53)	911 (±61)	906 (±74)
TN [mg L <sup>-1</sup> ]	147 (±13)	138 (±17)	145 (±9)	140 (±11)	134 (±14)	136 (±12)	136 (±8)	175 (±11)	173 (±8)	186 (±7)	147 (±13)
SRT [days]	27						14				

174

175 When steady state conditions were reached in both the SBRs, salt concentration was gradually  
 176 increased. In details, although steady state condition is conventionally referred to the SRT, in this  
 177 study it was assumed that steady state condition were reached when a steady nutrients removal  
 178 efficiency occurred (fluctuations smaller than 3%). Nevertheless, a minimum duration of 15 days



179 for each phase was imposed. The experiment was divided into eleven phases, during which salinity  
180 was stepwise increased by 2 gNaCl L<sup>-1</sup> each, by adding a known amount of sodium chloride to the  
181 diluted wastewater. In this way, the BOD<sub>5</sub> and total nitrogen concentration in the feed were kept  
182 constant during the entire experiment. Salinity was increased up to 50 gNaCl L<sup>-1</sup> and it was not  
183 further increased because of issues related to the oxygen transfer and scaling as a consequence of  
184 the high salt concentration.

185 The SRT was not imposed until Phase 6, corresponding to 40 gNaCl L<sup>-1</sup> (Table 1) when the sludge  
186 wastage flux was set in order to maintain a TSS concentration of approximately 12.0 gTSS L<sup>-1</sup> and  
187 6.0 gTSS L<sup>-1</sup> in the AGS-SBR and AS-SBR, respectively. Thus, the SRT was approximately of 27  
188 days in both the SBRs. However, due to the accumulation of inert material within the aerobic  
189 granules in the AGS-SBR and to the ageing of the activated sludge in the AS-SBR, since Phase 7 a  
190 regular sludge withdrawal, corresponding to a SRT close to 14 days, was performed. More  
191 precisely, a selective wastage strategy was performed in the AGS-SBR, consisting in discharging  
192 the granules from the bottom of the reactor after the settling phase. In this way, the heaviest  
193 granules, likely those with the highest inert matter content, were selectively wasted. In the AS-SBR  
194 the sludge was wasted from the liquid bulk during the aeration phase.

195 In Table 1.1 the main operating conditions and wastewater characteristics are summarized.

196

### 197 *2.3 Analytical methods*

198 The chemical-physical parameters (COD, BOD<sub>5</sub>, NH<sub>4</sub>-N, NO<sub>2</sub>-N) were analyzed according to  
199 standard methods (APHA, 2005). The TSS and volatile suspended solid (VSS) concentrations were  
200 troublesome due to the salt adsorption within the activated sludge flocs. To address this problem, a  
201 modified method was used (Capodici et al., 2018). The total nitrogen concentration was determined  
202 in Total Nitrogen Measuring Unit TNM-1 (Shimadzu, Japan).

203 EPS extraction was performed according to the heating method (Le-Clech et al., 2006). For each  
204 EPS fraction, the carbohydrates (PS) and the proteins (PN) were determined in accordance with the

205 phenol–sulfuric acid method (DuBois et al., 1956) and with the Folin method (Lowry et al., 1951),  
206 respectively.

207 The observed yield coefficient ( $Y_{obs}$ ) was calculated through mass balances between sludge  
208 withdrawn and sludge production, dividing by the cumulated  $BOD_5$  removed, according to Eq. 1:

$$210 \quad Y_{obs} = \frac{[(X_2 - X_1)V + X_e Q + X_s Q_s]}{(BOD_{in} - BOD_{out})Q} \quad [gVSS \ gBOD^{-1}] \quad (Eq. 1)$$

211  
212 where  $X_2$  and  $X_1$  are the biomass concentrations ( $g \ VSS \ L^{-1}$ ) at day (n) and (n-1), V is the working  
213 volume of the reactor, Q is the influent flow,  $X_s$  and  $X_e$  are the concentrations of the waste biomass  
214 and the effluent ( $g \ VSS \ L^{-1}$ ),  $Q_s$  is the volume of waste sludge on a daily base,  $BOD_{in}$  and  $BOD_{out}$   
215 are the influent and effluent  $BOD_5$  concentration ( $g \ L^{-1}$ ), respectively.

216 The size of the activated sludge flocs and granules was examined by means of a high-speed image  
217 analyses sensor (Sympatec Qicpic) that allowed the evaluation of sludge particle size distribution  
218 (PSD). The settling properties of the AGS and the AS were evaluated by means of the sludge  
219 volume index (SVI). The SVI was calculated as the ratio between the volume occupied by the  
220 sludge after a static settling phase and the TSS concentration of the sample. Because of the different  
221 nature of the AGS and AS, to compare the achieved results with previous respective studies, the  
222 SVI was calculated in a different way. More precisely, for the AGS the SVI was calculated based  
223 on the volume of settled sludge after 5 minutes ( $SVI_5$ ), whereas for the AS the SVI was calculated  
224 by considering the volume of settled sludge after 30 minutes ( $SVI_{30}$ ) (Giesen et al., 2013). The  
225  $SVI_{30}$  was calculated also for the AGS in order to evaluate the  $SVI_5/SVI_{30}$  ratio.

226 The dissolved oxygen (DO) concentration in the mixed liquor was measured continuously by means  
227 of a WTW IQ Sensor Net System 2020 XT equipped with on line sensor probes. The electrical  
228 conductivity (EC) was measured instead of a direct assessment of salinity, because it was more  
229 reliable. Therefore, salinity was calculated based on a correlation curve with the EC.

230 One-way analysis of variance (one-way ANOVA) was used to assess the relationship between  
231 salinity changes and biomass kinetics (error level equal to 0.05).

232

### 233 *2.3.1 Metabolic kinetic assessment*

234 To evaluate the impact of the salinity increase on nitrogen removal kinetics, ammonium utilization  
235 rate (AUR) and nitrite utilization rate (NUR) tests were performed in each experimental phase.  
236 Kinetic tests were performed only when steady conditions were reached. These tests were  
237 performed in a 1.5 L batch reactor (3 gTSS L<sup>-1</sup>) at controlled temperature (20°C). Specifically,  
238 based on the TSS concentration, a known amount of mixed liquor sample was withdrawn from the  
239 respective parent reactors and put in the batch reactor. Ammonium chloride and sodium nitrite were  
240 added as ammonia and nitrite sources respectively. Kinetic batch tests were replicated during each  
241 experimental phase.

242 During AUR tests DO was provided via a fine bubble diffuser and it was maintained close to the  
243 saturation value (in accordance with the temperature and salinity). NUR tests were performed in  
244 not-aerated conditions by using a magnetic stirrer device to mix the sample during the trials.  
245 Although anoxic conditions generally occur within the inner layers of granules even in the presence  
246 of dissolved oxygen in the bulk, it was decided to perform NUR tests for the AGS under the same  
247 conditions of the AS (not-aerated conditions). Sodium acetate was added as external carbon source  
248 to enhance the nitrites reduction. In particular, 100 ml of a concentrate solution containing sodium  
249 acetate (10 g L<sup>-1</sup>) was dosed as, to have a concentration within the batch reactor of approximately  
250 500 g L<sup>-1</sup>.

251 Moreover, in order to assess the possible presence of NOB, specific experiments were periodically  
252 run in a similar way than the AUR tests, by adding sodium nitrite instead of ammonium chloride  
253 under aerobic conditions.

254 Kinetic tests were operated for 2 hours each, during which 10 mL of sample was withdrawn at  
255 regular time intervals (10 minutes). Thus, samples were filtered through a 0.45µm membrane for

256 NH<sub>4</sub>-N and NO<sub>2</sub>-N analyses. The AUR and NUR were calculated as the slope of the linear  
257 regression line of NH<sub>4</sub>-N and NO<sub>2</sub>-N data. These values were then referred to the volatile suspended  
258 solids concentration of the sample. The initial ammonium concentration for each AUR batch test  
259 was approximately of 100 mg NH<sub>4</sub>-N L<sup>-1</sup>, whereas the nitrite concentration for the NUR tests was  
260 close to 50 mg NO<sub>2</sub>-N L<sup>-1</sup>.

261

### 262 *2.3.2 DNA extraction and 16S rRNA amplicon library preparation*

263 Samples (AGS-SBR and AS-SBR) for molecular analysis were collected at Phase 11 (salinity 50  
264 gNaCl L<sup>-1</sup>) to evaluate the bacterial composition of communities developed at the maximum  
265 salinity. DNA was extracted using the FastDNA Spin kit for soil (MP Biomedicals, Santa Ana, CA,  
266 USA). Bacterial 16S rRNA amplicon sequencing targeting the V1–V3 variable regions was  
267 performed following the procedure described by (Caporaso et al., 2010), using primers adapted  
268 from the Human Gut Consortium (Ward et al., 2012). Ten µl of extracted DNA were used as a  
269 template and the PCR reaction mix (25 µl) contained dNTPs (400nM of each), MgSO<sub>4</sub> (1.5 mM),  
270 Platinum® Taq DNA polymerase HF (2 mU), 1. Platinum® High Fidelity buffer (Thermo Fisher  
271 Scientific, Waltham, MA, USA), and barcoded library adaptors (400 nM) containing V1–3 specific  
272 primers: 27F AGAGTTTGATCCTGGCTCAG and 534R ATTACCGCGGCTGCTGG. PCR  
273 settings: initial denaturation at 95°C for 2 min, 30 cycles of 95°C for 20 s, 56°C for 30 s, 72°C for  
274 60 s and final elongation at 72°C for 5 min. All PCR reactions were run in duplicate and then  
275 pooled. The amplicon libraries were purified using the Agencourt® AMPure XP bead protocol  
276 (Beckmann Coulter, Indianapolis, IN, USA). The library DNA concentration was measured with the  
277 Quant-iT™ HS DNA Assay (Thermo Fisher Scientific) and quality validated with a TapeStation  
278 2200, using D1 K ScreenTapes (Agilent, Foster City, CA, USA). Based on library concentrations  
279 and calculated amplicon sizes, the samples were pooled in equimolar concentrations and diluted to 4  
280 nM.

281

### 282 2.3.3 DNA sequencing 16S rRNA amplicon bioinformatic processing

283 The samples were paired end sequenced (2.301 bp) on a MiSeq (Illumina, San Diego, CA, USA)  
284 using a MiSeq Reagent kit v3, 600 cycles (Illumina) following the manufacturer's guidelines for  
285 preparing and loading samples on the MiSeq. A 10% Phix control library was added to overcome  
286 low complexity issues often observed with amplicon samples (Illumina & Control). Forward and  
287 reverse reads were trimmed for quality using Trimmomatic v. 0.32 (Bolger et al., 2014) with the  
288 settings SLIDINGWINDOW:5:3 and MINLEN:275, and merged using FLASH v. 1.2.7 (Magoč  
289 and Salzberg, 2011), with the settings -m 25 -M 200. They were then de-replicated and formatted  
290 for use in the UPARSE workflow (Edgar, 2013) and clustered, using the usearch v. 7.0.1090 -  
291 cluster\_otus command with default settings. OTU abundances were estimated using the usearch v.  
292 7.0.1090 usearch\_global command with -id 0.97. Taxonomic status for each was assigned using the  
293 RDP classifier (Wang et al., 2007) as implemented in the parallel\_assign\_taxonomy\_rdp.py script  
294 in QIIME (Caporaso et al., 2010), using the MiDAS database v.1.20 (McIlroy et al., 2015). The  
295 results were analyzed in R (R Core Team 2015) through the Rstudio IDE using the ampvis package  
296 v.1.24.0 (Albertsen et al., 2015). Microbial community diversity was estimated by applying  
297 richness, Shannon and Simpson indices (Hill family indices) (Hill, 1973). Data analyses were  
298 performed with the software PAST (PAleontological STatistics).

299

## 300 **3. Results**

### 301 3.1 Granules and activated sludge characteristics

302 Physical properties of granular and activated sludge observed at different salinity are reported in  
303 Table 2.

304

305

306

307

**Tab. 2:** Physical properties of granular and activated sludge at different salinity.

Parameter	Phase	1	2	3	4	5	6	7	8	9	10	11	
	SRT	27						14					
	Salinity gNaCl L <sup>-1</sup>	30	32	34	36	38	40	42	44	46	48	50	
Mean size µm	AGS-SBR	2632 (±215)	2754 (±312)	2901 (±196)	3054 (±307)	3654 (±298)	3821 (±265)	2547 (±138)	2489 (±176)	2601 (±201)	2578 (±217)	2714 (±314)	
	AS-SBR	152 (±28)	136 (±35)	145 (±31)	151 (±17)	148 (±15)	132 (±28)	127 (±19)	119 (±16)	121 (±23)	123 (±17)	115 (±21)	
MLVSS g L <sup>-1</sup>	AGS-SBR	8.8 (±0.20)	8.77 (±0.35)	7.6 (±0.31)	7.17 (±0.24)	6.82 (±0.19)	5.92 (±0.31)	5.64 (±0.26)	6.18 (±0.17)	5.91 (±0.12)	6.2 (±0.09)	6.23 (±0.18)	
	AS-SBR	5.1 (±0.10)	4.8 (±0.24)	4.8 (±0.36)	4.66 (±0.41)	4.41 (±0.24)	4.32 (±0.29)	4.59 (±0.31)	4.78 (±0.19)	4.7 (±0.15)	4.49 (±0.11)	4.51 (±0.23)	
VSS/TSS %	AGS-SBR	66% (±2)	63% (±1)	60% (±3)	60% (±2)	59% (±1)	53% (±2)	54% (±2)	58% (±2)	66% (±1)	64% (±2)	65% (±3)	
	AS-SBR	84% (±3)	90% (±2)	86% (±1)	76% (±2)	70% (±2)	65% (±3)	71% (±2)	75% (±3)	75% (±2)	73% (±2)	73% (±2)	
SVI* mL gTSS <sup>-1</sup>	AGS-SBR	14.9 (±1.2)	16.2 (±1.9)	16.7 (±1.3)	16.9 (±2.1)	16.4 (±1.7)	18.3 (±2.4)	15.6 (±2.0)	15.1 (±1.7)	15.6 (±1.5)	16.1 (±1.9)	15.4 (±0.8)	
	AS-SBR	65.5 (±3.5)	69.5 (±4.2)	60.7 (±3.4)	45.5 (±2.7)	45.5 (±3.1)	37.5 (±3.4)	34.3 (±1.9)	35.6 (±1.7)	33.1 (±2.8)	34.9 (±4.1)	33.5 (±4.6)	
Yobs gVSS gBOD <sub>5</sub> <sup>-1</sup>	AGS-SBR	0.165 (±0.010)	0.181 (±0.006)	0.144 (±0.012)	0.160 (±0.017)	0.159 (±0.008)	0.153 (±0.022)	0.169 (±0.026)	0.151 (±0.016)	0.141 (±0.031)	0.118 (±0.014)	0.121 (±0.011)	
	AS-SBR	0.195 (±0.080)	0.178 (±0.033)	0.138 (±0.002)	0.135 (±0.014)	0.12 (±0.013)	0.113 (±0.017)	0.168 (±0.008)	0.159 (±0.016)	0.164 (±0.019)	0.159 (±0.020)	0.162 (±0.006)	

309 \*SVI<sub>5</sub> for AGS and SVI<sub>30</sub> for AS

310 Legend: MLVSS: Mixed Liquor Volatile Suspended Solids, VSS/TSS: volatile suspended solids/total suspended solids; SVI: Sludge Volume Index;

311 Yobs: Observed heterotrophic yield coefficient.

312

313 The mature granules obtained at the end of cultivation period were characterized by a mean size of  
314 approximately 2.6 mm, a SVI after 5 minutes of settling of 14.9 mL gTSS<sup>-1</sup> and an inert content of  
315 approximately 35% (VSS/TSS = 0.65). The mean size of granules rapidly increased during the  
316 experiment and granules of approximately 4 mm were obtained at 40 gNaCl L<sup>-1</sup> of salinity, which  
317 was consistent with previous studies that reported the average size of particles increased with  
318 salinity (Ji et al., 2018). Until Phase 6, the VSS concentration was decreasing and, accordingly, the  
319 inert content of the granules was over 45%, thereby indicating a significant accumulation of inert  
320 material. After the SRT was decreased to 14 days (Phase 7 onward) the VSS concentration and the  
321 VSS/TSS ratio increased to 65%, thereby suggesting the occurrence of biomass renewing.

322 The mean size of flocs in the AS-SBR slightly decreased with the increase in salinity from 152 µm  
323 to approximately 115 µm at 50 gNaCl L<sup>-1</sup> of salinity. The VSS concentration in the AS-SBR  
324 decreased during the period in which the SRT was maintained at approximately 27 days, reaching a  
325 minimum value of 4.32 gVSS L<sup>-1</sup> at Phase 6, corresponding to an inert content of 35%. After the  
326 SRT was decreased, the VSS concentration ranged between 4.5 gVSS L<sup>-1</sup> and 4.7 gVSS L<sup>-1</sup> until the  
327 end of the experiment. The inert content was close to 27% and it was constant for the rest of the

328 experiment, thereby indicating that salt accumulation within the flocs did not occurred under lower  
329 SRT.

330 Referring to the SVI values, no significant changes with the increase in salinity were observed in  
331 the AGS-SBR. The SVI<sub>5</sub> slightly ranged between 14 mL gTSS<sup>-1</sup> and 17 mL gTSS<sup>-1</sup> during the entire  
332 experiment, whereas the SVI<sub>5</sub>/SVI<sub>30</sub> value was approximately 1.1. This result was in contrast with  
333 the findings of a previous study in which the SVI decreasing with the increase in salinity (from 2  
334 gNaCl L<sup>-1</sup> to 15 gNaCl L<sup>-1</sup>) (Wang et al., 2017). This was probably due to the fact that in this study  
335 the maturation of granular sludge was achieved before than salinity was increased, whereas in the  
336 study by Wang and co-authors, salinity was increased simultaneously with the granulation process.

337 The SVI<sub>30</sub> decreased with the increase in salinity in the AS-SBR. Starting from an initial value of 85  
338 mL gTSS<sup>-1</sup>, the SVI<sub>30</sub> constantly decreased to 68 mL gTSS<sup>-1</sup> at the end of the experiment. This  
339 result could be related to the increase of the bulk buoyancy that resulted in the increase of the  
340 hydraulic selection pressure. In this way, the reactor started to enrich in faster-settling activated  
341 sludge. Similar findings were also achieved in other studies (Chen et al., 2018; Ou et al., 2018a).  
342 This was not observed in the AGS-SBR likely because the granules were already hydraulically-  
343 selected by the shorter duration of the settling phase.

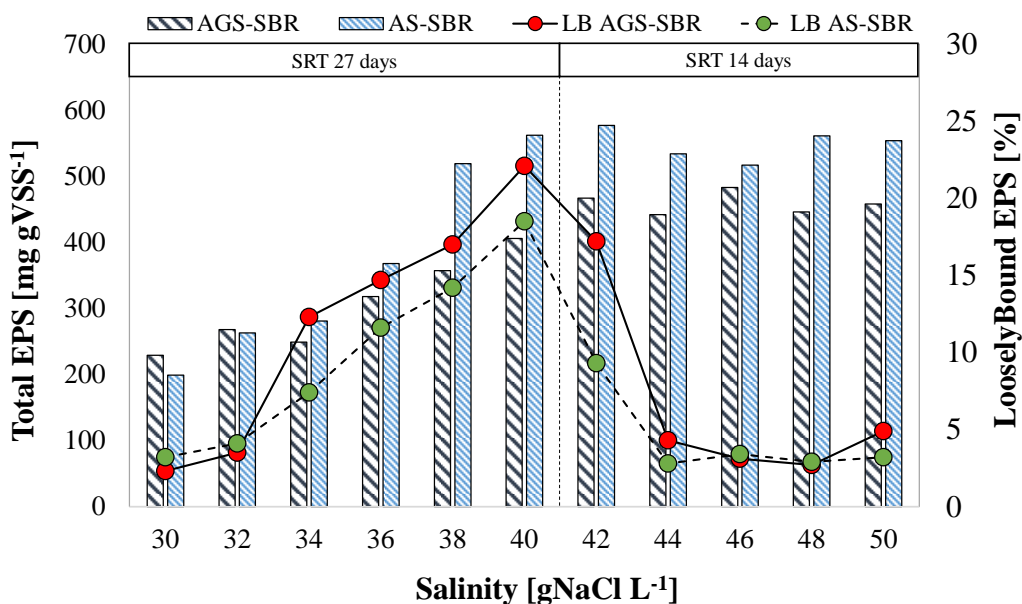
344 The observed yield coefficient of the heterotrophic biomass in the AGS-SBR slightly decreased  
345 during the entire experiment from 0.168 gVSS g BOD<sub>5</sub><sup>-1</sup> to 0.121 gVSS g BOD<sub>5</sub><sup>-1</sup>, suggesting the  
346 reduction of new biomass synthesis due to the salinity increase, which was consistent with the  
347 literature (Mannina et al., 2016; Wu et al., 2008). The influence of SRT on the observed yield  
348 coefficient resulted negligible. Similarly, in the AS-SBR the observed yield coefficient decreased  
349 by almost 40%, from 0.195 gVSS g BOD<sub>5</sub><sup>-1</sup> (Phase 1) to 0.113 gVSS g BOD<sub>5</sub><sup>-1</sup> at salinity of 40  
350 gNaCl L<sup>-1</sup>. However, after Phase 7 (42 gNaCl L<sup>-1</sup>), under SRT of 14 days, the Y<sub>obs</sub> increased and  
351 ranged between approximately 0.159 gVSS g BOD<sub>5</sub><sup>-1</sup> and 0.168 gVSS g BOD<sub>5</sub><sup>-1</sup> until the end of the  
352 experiment.

353 The achieved results indicated that the biomass synthesis decreased with the increase in salinity.  
 354 Nevertheless, a lower SRT enhanced the biomass renewing, as well as the synthesis of new  
 355 bacterial cells. It is reasonable to explain the biomass activity although the high salinity level due to  
 356 the dominance of the marine species.

357

### 358 3.2 EPS pattern in activated and granular sludge

359 The trend of the specific EPS content and that of the loosely-bound fraction in the activated sludge  
 360 and granular sludge reactors during the experiment are depicted in Fig. 1.



361

362 *Legend:* AGS-SBR: Bound EPS in the AGS reactor; AS-SBR: Bound EPS in the AS reactor;  
 363 LB AGS-SBR: Loosely Bound EPS in the AGS reactor; LB AS-SBR: Loosely Bound EPS in the AS reactor;

364

365 **Fig.1:** Trends of the specific EPS content and percentage of loosely-bound EPS in the activated  
 366 sludge (AS) and granular sludge (AGS) reactors.

367

368  
 369 The specific EPS content increased with salinity in both the SBRs, thereby confirming that bacteria  
 370 produce excess of exopolymers to face the salinity increases (Corsino et al., 2017; Ji et al., 2018).

371 This is likely due to the cell protection role played by EPS against high salinity, as suggested for  
 372 biofilm communities (Decho, 2013). These exopolymeric substances are an abundant component of



373 microbial mats developed in hypersaline systems, such as salt ponds, salterns and hypersaline  
374 lagoons (Decho and Gutierrez, 2017), where EPS seem to condense with increasing salinity and  
375 even form a hydrophobic barrier on the surface of biofilm (Decho, 2013).

376 Interestingly, the EPS content significantly started to increase in both the reactors after Phase 4,  
377 when the salinity was equal to 36 gNaCl L<sup>-1</sup>. In general, when saline concentration is changing in  
378 the bulk, the overproduction of EPS helps to reduce the destruction of microorganisms due to  
379 maintaining of the cellular osmotic pressure balance. In halotolerant-activated sludge bioreactors,  
380 the response of bacteria to salinity increases, in terms of overproduction of EPS, occurs from  
381 salinity levels of approximately 5-10 gNaCl L<sup>-1</sup> (Campo et al., 2018; Wang et al., 2015). In this  
382 study, the response by the halophilic marine bacteria to the salinity increase occurred at salinity  
383 over 36 gNaCl L<sup>-1</sup>. Therefore, based on the result above, it is possible to speculate that the response  
384 of marine bacteria to the salinity increase, in terms of overproduction of EPS, started when the  
385 gradient of osmotic pressure between the inner and the outer of the bacterial cells exceeded a certain  
386 threshold value which is significantly higher than that of halotolerant microorganisms.

387 In both the AGS-SBR and the AS-SBR, the EPS were mainly constituted by the tightly-bound  
388 fraction (average value >90%). However, it is worth to observe that the loosely bound fraction was  
389 increasing when the SRT was not controlled (Fig. 1). Indeed, the loosely bound fraction reached its  
390 maximum value at Phase 6 in both the reactors, when the salinity was equal to 40 gNaCl L<sup>-1</sup>.  
391 Specifically, the LB-EPS accounted for approximately 22% and 18% of the total EPS content in the  
392 AGS-SBR and AS-SBR, respectively. This result was in good agreement with a previous study  
393 (Corsino et al., 2017), in which the authors observed an exponential increase in the LB-EPS content  
394 with the increase in salinity under not controlled SRT. After Phase 6, when a shorter SRT was  
395 applied, the LB-EPS fraction decreased in both the reactors as far as a stable value of approximately  
396 5% in the AGS-SBR and 3% in the AS-SBR was reached. Previous studies demonstrated that the  
397 increase in salinity caused a significant increase in the loosely-bound EPS fraction of halotolerant  
398 activated and granular sludge (Corsino et al., 2017; Wang et al., 2015; L. Zhao et al., 2016).

399 Similarly, other authors observed a significant increase in the loosely-bound EPS of halophilic  
400 biomass, in both forms of activated and granular sludge, subjected to drastic salinity increase  
401 (Corsino et al., 2018). Ismail et al. (2010) demonstrated that under high salinity the EPSs matrix  
402 suffers a deterioration, because of the replacement of calcium ions by sodium ones, thereby  
403 resulting in the increase in the loosely-bound fraction. In contrast, the results obtained in this study  
404 indicated that by stepwise increasing the salinity and by decreasing the SRT, the amount of loosely-  
405 bound EPS decreased. These results likely suggest that the detrimental effect exerted by sodium  
406 cations toward the EPS matrix occurs in the long-term and as a response of high salinity increases.  
407 Therefore, lower SRT and stepwise salinity increases enable to minimize the EPS matrix  
408 deterioration, thereby promoting the formation of sludge with good physical characteristics.

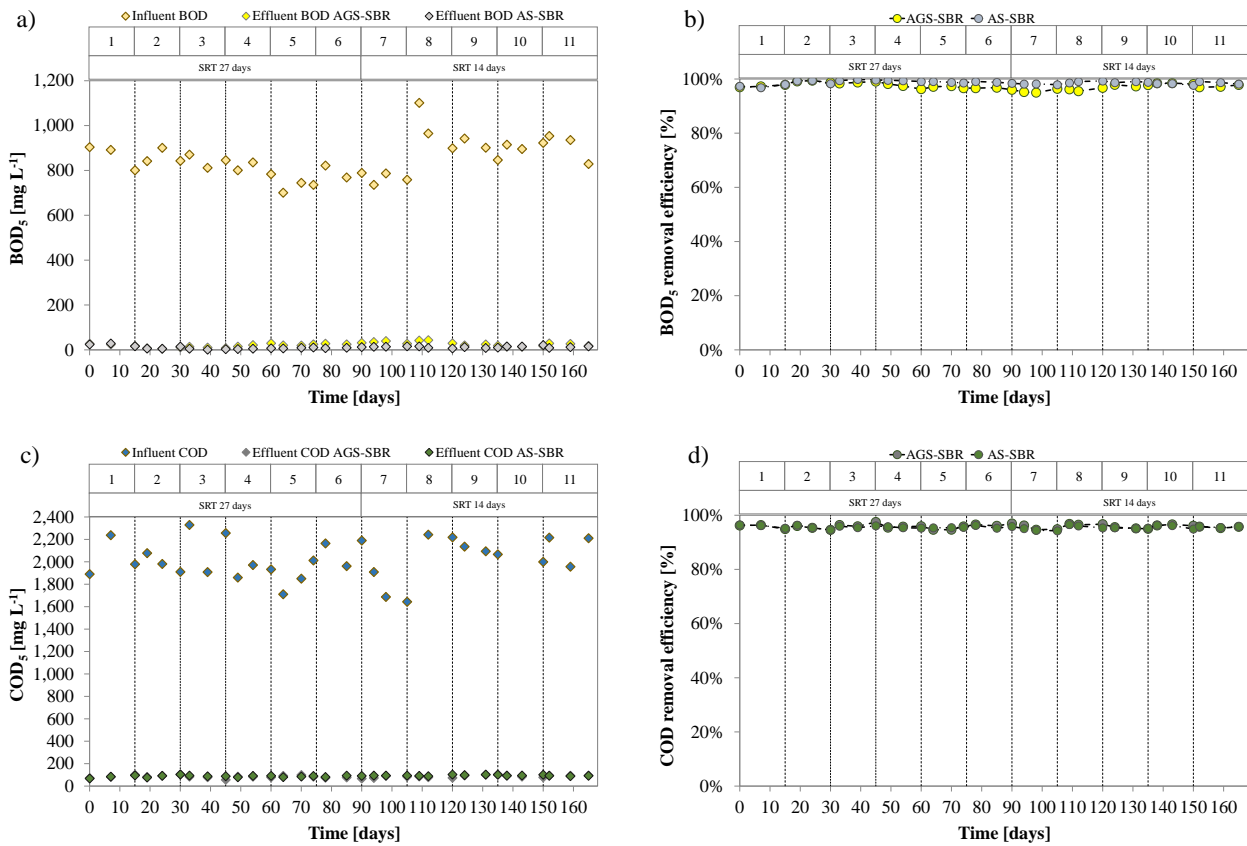
409 Concerning the EPS composition, the proteins resulted the main EPS constituent. The amount of  
410 proteins was more than five times higher than that of carbohydrates and no significant changes were  
411 observed in the PN/PS ratio with the increase in salinity and SRT as well. Specifically, the protein  
412 concentration increased from 190 mg gVSS<sup>-1</sup> to approximately 320 mg gVSS<sup>-1</sup> in the AGS and from  
413 150 mg gVSS<sup>-1</sup> to approximately 410 mg gVSS<sup>-1</sup> in the AS during the entire experiment. Similarly,  
414 the carbohydrates concentration increased from 40 mg gVSS<sup>-1</sup> to approximately 65 mg gVSS<sup>-1</sup> in  
415 the AGS and from 30 mg gVSS<sup>-1</sup> to approximately 82 mg gVSS<sup>-1</sup> in the AS during the entire  
416 experiment. Consequently, the PN/PS ratio was constant to a stable value of approximately 5 during  
417 the entire experiment.

418

### 419 *3.3 Carbon removal efficiency*

420 Time courses of the BOD<sub>5</sub> and COD in the influent and effluents of the AGS-SBR and AS-SBR, as  
421 well as the removal efficiencies in both the reactors are depicted in Fig. 2a and Fig. 2b, respectively.

422



423

424 **Fig.2:** Influent and effluent concentrations for BOD (a) and COD (c) and the removal efficiencies  
 425 (b,d) during the eleven experimental phases.

426

427 The BOD<sub>5</sub> in the influent fish canning wastewater ranged approximately between 700 mg L<sup>-1</sup> and  
 428 1100 mg L<sup>-1</sup>. Both the SBRs provided effluents of constant quality in terms of BOD<sub>5</sub>, which  
 429 resulted always below 45 mg L<sup>-1</sup> and 30 mg L<sup>-1</sup> in the AGS-SBR and AS-SBR, respectively.  
 430 Therefore, the carbon removal efficiency was on average equal approximately to 98%, which was  
 431 much higher than the performance achieved in other studies with salt-adapted microorganisms  
 432 (Chen et al., 2018; Ou et al., 2018a). A slight decrease was observed in both reactors when the SRT  
 433 was set equal to 27 days, likely due to the accumulation of salt within the flocs and granules as  
 434 discussed above. The reduction of SRT since Phase 7 enabled the biomass renewing, resulting in an  
 435 improvement of carbon removal efficiency. The removal efficiencies in both the reactors were in  
 436 good agreement with the VSS/TSS ratio values (Table 1), suggesting that when treating saline

437 wastewater a lower SRT enables to avoid the decrease of the active biomass within the microbial  
438 aggregates, thereby preventing the worsening of the biological performances.

439 A similar trend was observed also concerning the COD. The COD in the influent ranged between  
440 1710 mg L<sup>-1</sup> and 2423 mg L<sup>-1</sup>, whereas the COD in the effluent was mostly below 100 mg L<sup>-1</sup> in  
441 both the AGS and the AS systems (Fig. 2c). Overall, both the SBRs provided more than 95% of  
442 COD removal. The achieved results indicated that the autochthonous heterotrophic bacteria were  
443 extremely active even at high salinity levels. In terms of organic loading rate, both the SBRs were  
444 able to remove more than 95% of the influent organic load with an average rate of approximately  
445 2.14 g COD m<sup>-3</sup>d<sup>-1</sup>. In a previous study, Zhao et al. (Zhao et al., 2016) obtained 80% of COD  
446 removal at 35 gNaCl L<sup>-1</sup> in a SBR with acclimated activated sludge operating with an organic  
447 loading rate of approximately 2 g COD m<sup>-3</sup>d<sup>-1</sup> (synthetic medium). Similarly, in an salt-adapted  
448 AGS system, Ou et al. (Ou et al., 2018b) achieved the removal of approximately 1.06 g COD m<sup>-3</sup>d<sup>-1</sup>  
449 operating with acetate-based wastewater at 50 gNaCl L<sup>-1</sup> of salinity. Based on the available  
450 literature, salt-adapted microorganisms were able to remove approximately the 50-70% of the  
451 influent organic load at salinity higher than 30 gNaCl L<sup>-1</sup>, showing a decreasing trend with the  
452 salinity increase (Ji et al., 2018; Wang et al., 2014). It is worth mentioning that mostly of the cited  
453 studies are referred to the treatment of synthetic wastewater. While referring to real wastewater, Val  
454 del Río et al. (Val del Río et al., 2012) obtained the removal approximately of 30% of the influent  
455 organic loading rate (4 g COD m<sup>-3</sup>d<sup>-1</sup>) in a AGS-SBR treating fish-canning wastewater at 30 gNaCl  
456 L<sup>-1</sup> of salinity. Similarly, Figueroa et al. (Figueroa et al., 2008) obtained 90% of COD removal in a  
457 AGS-SBR operating with an organic loading rate of 1.5 g COD m<sup>-3</sup>d<sup>-1</sup> at 30 gNaCl L<sup>-1</sup> of salinity  
458 after a long acclimation period.

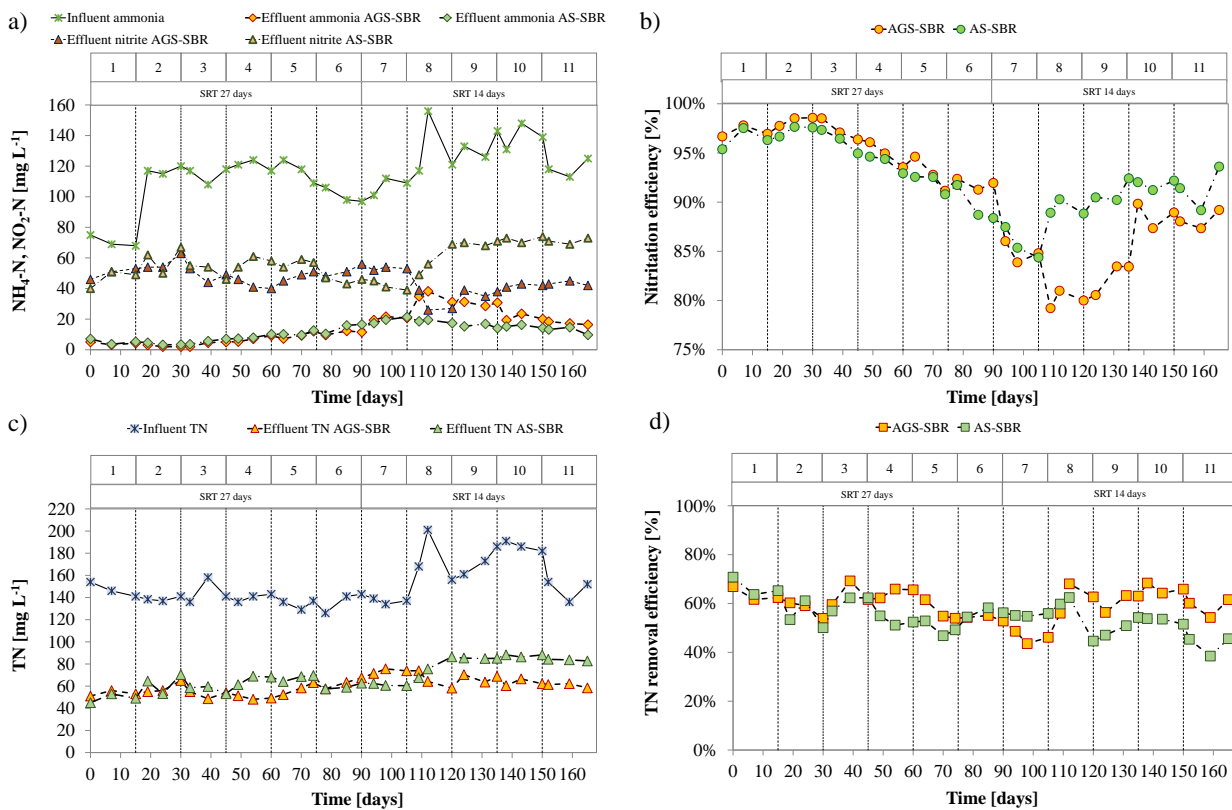
459 The results achieved in this study demonstrated that the autochthonous marine biomass was able of  
460 providing excellent carbon removal performance even at higher salinity than those tested in  
461 previous studies (Capodici et al., 2018; Ramos et al., 2015; van den Akker et al., 2015). The  
462 dominance of this marine species can explain the biomass activity although the high salinity level. It

463 is worth mentioning that strategy of stepwise increasing the salinity contributed to avoid sudden  
 464 increase in the solute concentration around bacterial cells, thereby preventing osmotic stress.  
 465 Indeed, drastic osmotic shocks would cause plasmolysis because cells lose water through osmosis,  
 466 thus inhibiting the transport of substrates into the cell and the carbon removal performance (Lang et  
 467 al., 2005). A gradual adaptation to salinity enables bacteria to face to the higher osmotic pressure by  
 468 accumulating organic compounds in the cytoplasm, avoiding the loss of the metabolic activity.  
 469 The obtained results clearly demonstrated that the use of autochthonous biomass and the stepwise  
 470 increase in salinity are effective approaches to achieve excellent carbon removal performance for  
 471 the treatment of wastewater at high salinity.

472

### 473 3.4 Nitrogen removal efficiency

474 The overall performance of AGS-SBR and AS-SBR systems concerning nitrogen removal with the  
 475 increased salinity is shown in Fig.4.

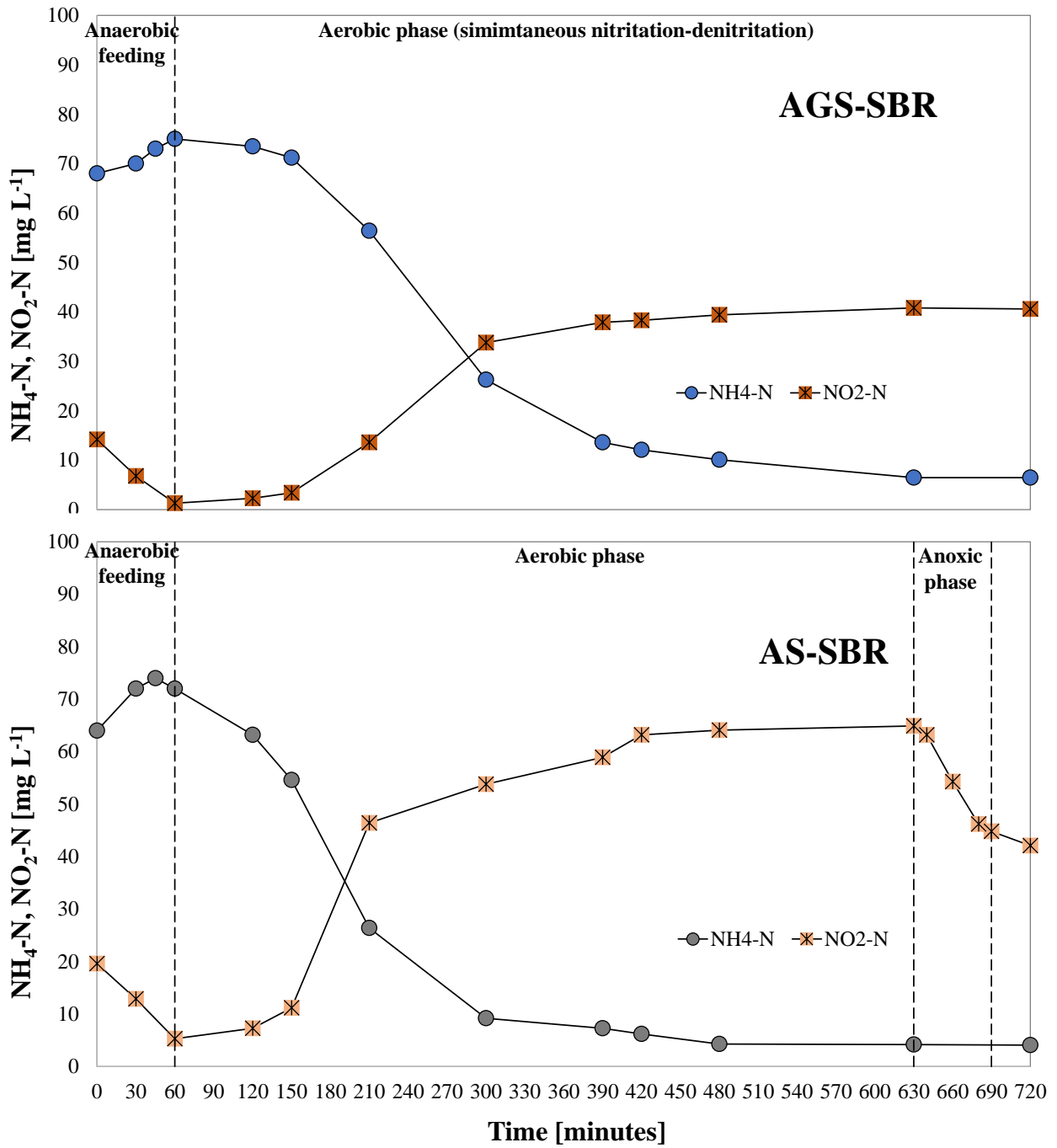


476

477 **Fig.3:** Influent and effluent concentrations of the ammonium and nitrite in the AGS-SBR and AS-  
478 SBR (a) and nitrification efficiency (b) at different salinity; influent and effluent concentrations of TN  
479 (c) and removal efficiencies (d).

480

481 In this study no nitrates were observed in the effluent for the entire experiment, and also kinetic  
482 batch tests confirmed that biological activity of NOB bacteria was inhibited in high-saline  
483 environment. Besides, also NGS analysis revealed the absence of NOB bacteria in both the SBRs  
484 communities. A typical trend of the nitrogen pattern during an operational cycle in the AGS-SBR  
485 and AS-SBR (Phase 1) is shown in Fig. S1.



486

487 **Fig.S1:** Trends of ammonium and nitrite during a typical SBR cycle in the AGS and AS systems

488

(Phase 1)

489

490 Since the SRT was set equal to 27 days, the effluent ammonium concentration showed a slightly

491 increasing trend in both the SBRs, while maintaining always below 20 mg L<sup>-1</sup> (Fig. 3a).

492 Accordingly, the nitrification efficiencies decreased from approximately 98% (Phase 1) to 92% and

493 88% in the AGS-SBR and AS-SBR, respectively (Fig. 3b). The achieved results were in good  
494 agreement with the sludge ageing previously discussed. Nevertheless, the nitrification performance  
495 was approximately close to 90% in both the SBRs, thereby indicating a high activity of the Beta-  
496 AOB, mainly belonging to *Nitrosomonas* species, as shown by NGS analysis.

497 When the SRT was decreased at the beginning of Phase 7, the effluent ammonium concentration  
498 increased in both the reactors. In particular, the effluent ammonium concentration reached its  
499 maximum value at Phase 8 of approximately 36 mg L<sup>-1</sup> and 23 mg L<sup>-1</sup> in the AGS-SBR and AS-  
500 SBR, respectively. Accordingly, the nitrification efficiency rapidly decreased, reaching the minimum  
501 value of 78% in the AGS-SBR and 85% in the AS-SBR. This result could be likely related to the  
502 SRT decrease, which caused a wash-out of nitrifiers. Nevertheless, both the reactors rapidly adapted  
503 to the new operating conditions. Indeed, the effluent ammonium concentration decreased in the  
504 subsequent phases, reaching a steady value of approximately 18 mgNH<sub>4</sub>-N L<sup>-1</sup>. At the end of the  
505 experiment, the nitrification efficiency was 93% and 88% in the AGS-SBR and AS-SBR,  
506 respectively. Based on the achieved results, the salinity did not significantly affect the biological  
507 activity of the halophilic AOB strains, which were able to provide high performances during the  
508 entire experiment. In contrast, an excessive accumulation of salt and inert material within the  
509 granules or flocs worsened the nitrification performances likely because of the decrease in the overall  
510 active biomass within the reactors that occurred from Phase 1 to Phase 6 before the SRT was  
511 decreased.

512 During the entire experiment, the nitrite concentrations in the effluents of the SBRs ranged between  
513 40 mg NO<sub>2</sub>-N L<sup>-1</sup> and 70 mg NO<sub>2</sub>-N L<sup>-1</sup> consistent with the ammonium oxidation performances.  
514 The high concentration of nitrites in the effluent suggested that the denitrification process was limited  
515 independently of salinity. Nitrites reduction by denitrifiers occurred during the anoxic period in the  
516 AS-SBR and within the layered structure of the granules in the AGS-SBR, simultaneously with the  
517 nitrification process (Corsino et al., 2016).

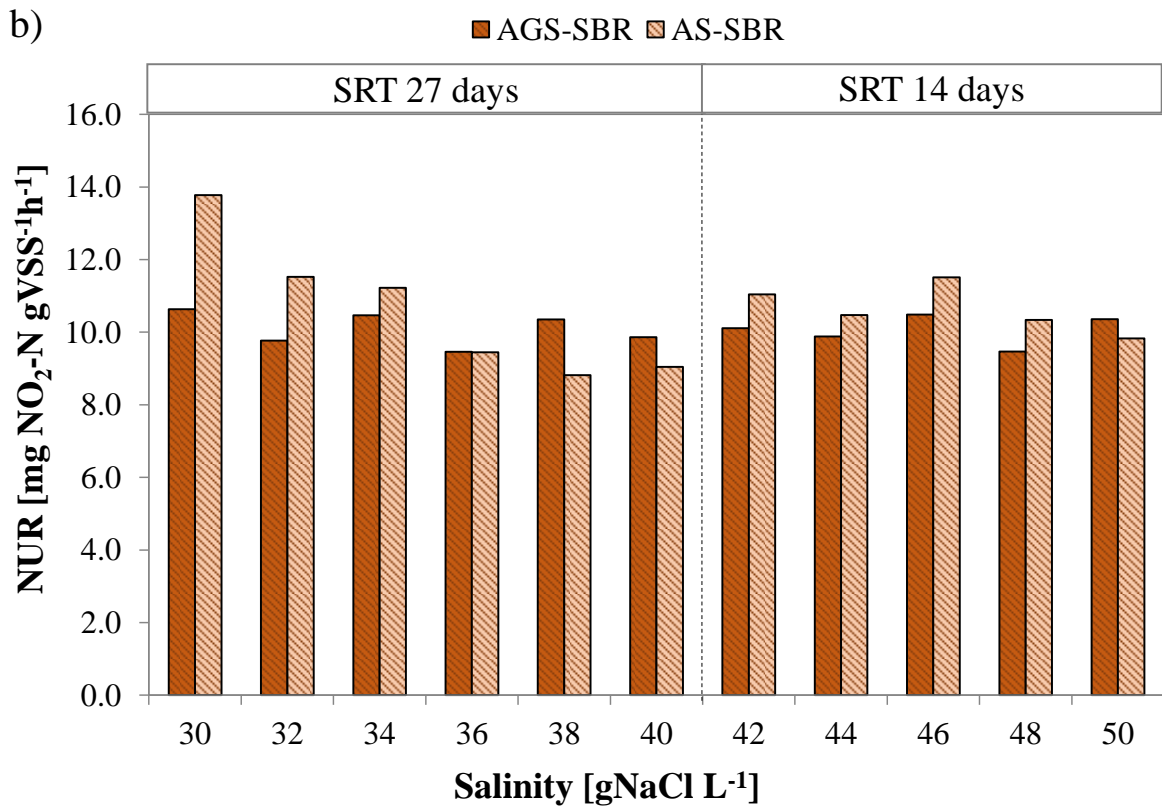
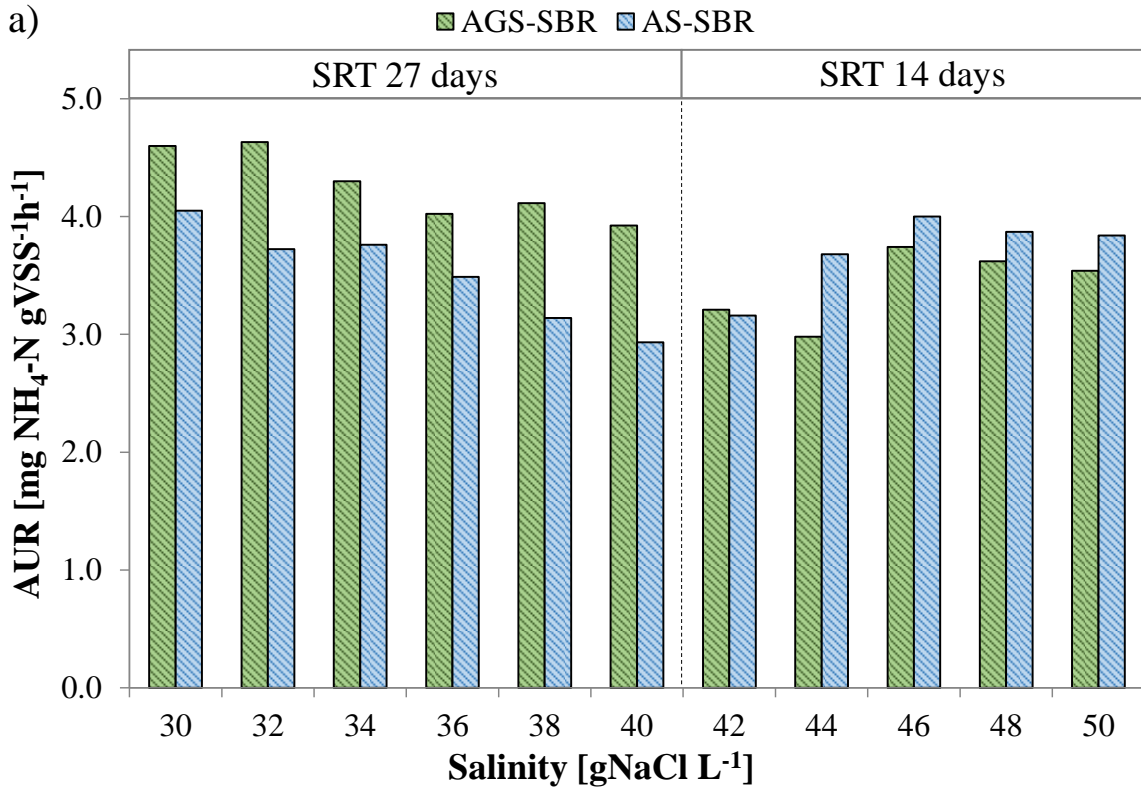


518 Overall, the total nitrogen concentration in the SBRs effluents ranged between 40 mg TN L<sup>-1</sup> and 75  
519 mg TN L<sup>-1</sup> (Fig. 3c), resulting in TN removal efficiencies ranging between 60% and 40% in the  
520 AGS-SBR and AS-SBR, respectively (Fig. 3d). No significant relation with the increase in salinity  
521 was observed. Based on the results above, denitrification was the limiting process for total nitrogen  
522 removal. It is reasonable to assume that denitrification was limited by lack of carbon as nitrite  
523 concentration in both the effluents did not show any significant relation with salinity. However, a  
524 distinction should be made between the AGS-SBR and the AS-SBR. In the latter, because  
525 denitrification occurred only during the not-aerated phase, when ammonium was already oxidized to  
526 nitrite and the organic carbon was almost completely oxidized. Therefore, this certainly limited the  
527 availability of the organic substrate for nitrite reduction. It is reasonable that endogenous  
528 denitrification occurred through the use of bacterial internal carbon sources that limited the reaction  
529 kinetic (Bernat et al., 2008). In the AGS reactor, in addition to the carbon limitation, it is also  
530 reasonable that the high oxygen concentration in the bulk, close to the saturation value, was the  
531 limiting factor for the simultaneous nitrification-denitrification process. Indeed, under these operating  
532 conditions, it is possible that the oxygen concentrations in the inner layers of the granule was very  
533 high, thereby favouring aerobic reactions instead of anoxic.

534

### 535 *3.5 Nitrogen removal kinetics*

536 Nitritation and denitrification kinetics were evaluated by means of AUR and NUR tests. The results  
537 obtained during the experiments are depicted in Fig. 4.



538

539 **Fig. 4:** Values of the ammonium utilization rate (a) and the nitrite utilization rate (b) in each Phase  
 540 of the experiment.

541

542 Nitritation and denitritation kinetics showed a high metabolic activity of both nitrifying and  
543 denitrifying bacteria although the high salinity level. The achieved results were comparable to those  
544 of CAS systems (Metcalf and Eddy, 2015) and were significantly higher than kinetics related to  
545 halotolerant biomass (Pronk et al., 2014).

546 AUR slightly decreased in both SBRs when salinity was increased from 30 gNaCl L<sup>-1</sup> to 40 gNaCl  
547 L<sup>-1</sup> (Fig. 4a) during the period at 27 days of SRT. More precisely, the AUR in the AGS-SBR  
548 decreased from 4.67 mgNH<sub>4</sub>-N gVSS<sup>-1</sup>h<sup>-1</sup> at 30 gNaCl L<sup>-1</sup> of salinity to 3.97 mgNH<sub>4</sub>-N gVSS<sup>-1</sup>h<sup>-1</sup> at  
549 salinity of 40 gNaCl L<sup>-1</sup>, thereby reducing by approximately 16%. In contrast, the AUR in the AS-  
550 SBR decreased from 4.05 mgNH<sub>4</sub>-N gVSS<sup>-1</sup>h<sup>-1</sup> to 2.93 mgNH<sub>4</sub>-N gVSS<sup>-1</sup>h<sup>-1</sup> within the same range  
551 of salinity. Thus, the decrease in AUR was of approximately 38% in the AS-SBR, which was 2.4  
552 times more the AGS-SBR. These results were in good agreement with nitritation performances  
553 above discussed.

554 Based on these results, the increase in salinity with a stepwise strategy within a range of 30 gNaCl  
555 L<sup>-1</sup> and 40 gNaCl L<sup>-1</sup> had a negligible effect on biological activity of AOBs in the AGS (i.e., p =  
556 0.286), whereas a significant decrease was noted in the AS, although the one-way analysis of  
557 variance indicated a low correlation value (i.e., p = 0.210).

558 After Phase 6, at salinity of 40 gNaCl L<sup>-1</sup>, the AUR sharply decreased in the AGS-SBR  
559 approximately by 22%. At salinity of 42 gNaCl L<sup>-1</sup> the AUR in the AGS-SBR was approximately  
560 3.20 mgNH<sub>4</sub>-N gVSS<sup>-1</sup>h<sup>-1</sup> and this value was comparable with that in the AS-SBR. Therefore, a  
561 sharp decrease in AOBs activity was noted at salinity higher than 40 gNaCl L<sup>-1</sup>, although this  
562 occurred only in the AGS reactor. Such result could be likely due to the accumulation of inert  
563 material within the granules and to the limitation to oxygen diffusion. Indeed, at Phase 6,  
564 approximately the 78% of aerobic granules were on average bigger than 4 mm, likely because of the  
565 inclusions of inert material within the structure of granules, (salt and inert particulate deriving from  
566 the raw wastewater). The high salt concentration that decreased the oxygen saturation within the  
567 liquid bulk, and the bigger size of granules, increased the resistance to oxygen diffusion within the

568 inner layers, endangering the ammonia oxidation process. Besides, accumulation of inert inorganic  
569 material within the granule caused a decrease in the VSS/TSS ratio that was approximately 53%.  
570 Because of the lower VSS/TSS ratio in the AGS, the biologically active fraction of the granule  
571 significantly decreased, thereby reducing the ammonium oxidation capacity by the AGS system.  
572 After the SRT was decreased to 14 days, the new operating conditions rapidly reflected on the  
573 AOBs activity in the AS-SBR. Indeed, the AUR increased from 3.18 mgNH<sub>4</sub>-N gVSS<sup>-1</sup>h<sup>-1</sup> to  
574 approximately 4.0 mgNH<sub>4</sub>-N gVSS<sup>-1</sup>h<sup>-1</sup> at salinity of 46 gNaCl L<sup>-1</sup>. Thereafter, the AUR ranged  
575 between 3.87 mgNH<sub>4</sub>-N gVSS<sup>-1</sup>h<sup>-1</sup> and 3.84 mgNH<sub>4</sub>-N gVSS<sup>-1</sup>h<sup>-1</sup> during the rest of the experiment.  
576 Contrarily, the AUR in the AGS-SBR still decreased until Phase 8 at salinity of 44 gNaCl L<sup>-1</sup>, when  
577 it reached its minimum value of approximately 2.44 mgNH<sub>4</sub>-N gVSS<sup>-1</sup>h<sup>-1</sup>. Subsequently, a reversal  
578 of this decreasing trend occurred. However, the trend reversal point was slightly shifted in time  
579 respect to that in the AS-SBR. In the last experimental Phase, at 50 gNaCl L<sup>-1</sup> of salinity, the AUR  
580 reached a value of approximately 3.54 mgNH<sub>4</sub>-N gVSS<sup>-1</sup>h<sup>-1</sup>. It is worth mentioning that the  
581 shortened in SRT after Phase 6, caused the decrease in the size of granules in the AGS-SBR. This  
582 certainly affected the AUR kinetics, because the smaller size of bio-aggregates favoured the  
583 increase of oxygen penetration depth, thereby increasing the aerobic zone of the granule which is  
584 associated with the capacity for nitrification (Wang et al., 2017).

585 Overall, the stepwise increase strategy resulted in a decrease in AUR of approximately 2.7% and  
586 0.5% in the AGS-SBR and AS-SBR respectively for each salinity increase. Nonetheless, the  
587 stepwise strategy of increasing salinity did not significantly affect the AUR kinetics of the AGS-  
588 SBR and AS-SBR systems. The results of one-way analysis of variance (one-way ANOVA)  
589 indicated that, considering the entire range of salinity, the salinity increase had a marginal effect on  
590 AUR kinetic in the AGS ( $p > 0.302$ ) and the AS reactors ( $p > 0.289$ ).

591 Based on the results above, the metabolic activity of the AOBs was higher in the AGS than the AS  
592 up to a salinity of 40 gNaCl L<sup>-1</sup>, whereas at higher salinity levels, AUR kinetics were higher in the  
593 AS. It is worth mentioning that over a certain salinity, the oxygen diffusion within the liquid bulk

594 began to be salt-limited (Zannotti and Giovannetti, 2015). Consequently, at high salinity, the  
595 ammonia oxidation process could be oxygen limiting. Besides, in the aerobic granules autotrophic  
596 bacteria develop in the inner layers (Winkler et al., 2012). Consequently, to provide enough electron  
597 donors for the AOBs metabolic functionalities, oxygen has to penetrate deeper within the granule.  
598 Therefore, although the compact structure of the granules act as a kind of protecting shield for  
599 bacteria, it makes even more difficult the oxygen diffusion within the inner layers. This would  
600 explain why over a salinity of 40 gNaCl L<sup>-1</sup> the metabolic activity of AOBs was higher in the AS-  
601 SBR. At lower salinity instead, the oxygen diffusion is not a limiting factor for the ammonia  
602 oxidation process. Therefore, within a range of salinity between 30 gNaCl L<sup>-1</sup> and 40 gNaCl L<sup>-1</sup>  
603 AUR kinetics were higher in the AGS-SBR likely because of the higher active biomass retention in  
604 the aerobic granules than the flocculent activated sludge that enabled to enhance a faster oxidation  
605 of ammonium. In this respect, the NUR tests confirmed that lower SRT enabled to achieve a  
606 significant reprise of metabolic activity of AOBs strains especially in AGS systems.

607 The values of the NUR at different salinity are shown in Figure 4b. The NUR ranged between 9  
608 mgNO<sub>2</sub>-N gVSS<sup>-1</sup>h<sup>-1</sup> and 10.5 mgNO<sub>2</sub>-N gVSS<sup>-1</sup>h<sup>-1</sup> in the AGS-SBR during the entire experiment,  
609 independently of salinity. Conversely, the NUR in the AS-SBR showed a decreasing trend during  
610 the period at SRT of 27 days, when salinity was increased from 30 gNaCl L<sup>-1</sup> to 40 gNaCl L<sup>-1</sup>.  
611 Indeed, the NUR decreased from 13.8 mgNO<sub>2</sub>-N gVSS<sup>-1</sup>h<sup>-1</sup> to approximately 9.0 mgNO<sub>2</sub>-N gVSS<sup>-1</sup>  
612 h<sup>-1</sup> at Phase 6 at salinity of 40 gNaCl L<sup>-1</sup>, thereby decreasing approximately of 40%. After Phase 6,  
613 when the SRT was decreased, the NUR in the AS-SBR increased and ranged between 9.8 mgNO<sub>2</sub>-  
614 N gVSS<sup>-1</sup>h<sup>-1</sup> and 11.5 mgNO<sub>2</sub>-N gVSS<sup>-1</sup>h<sup>-1</sup> until the end of the experiment.

615 Based on the results above, denitrifies activity was independent of both salinity and SRT in the  
616 AGS-SBR. Although the size of the granules decreased after Period 6, this did not affect the NUR  
617 kinetics of the AGS. Indeed, the average size of the granules was larger than 2.5 mm, thereby  
618 enabling the achievement of a sufficient anoxic zone within the granule structure that allowed the  
619 maintenance of the denitrification capacity.

620 Conversely, the NUR in the AS-SBR decreased with the increase in salinity until Phase 6 as  
621 previously observed for the AUR. However, the decrease of the SRT enabled a recovery of  
622 denitrifies metabolism independently of salinity. This result suggested that the biomass ageing in  
623 the AS-SBR occurred until Phase 6 caused a significant decrease in the heterotrophic active  
624 fraction, whereas a lower SRT allowed the biomass renewing. Indeed, it was calculated that the  
625 specific observed heterotrophic yield in the AS-SBR decreased with the increase in salinity from  
626  $0.20 \text{ gVSS gBOD}^{-1}$  to approximately  $0.10 \text{ gVSS gBOD}^{-1}$  at salinity of  $40 \text{ gNaCl L}^{-1}$ . Thereafter, the  
627 decrease in the SRT enabled to increase the  $Y_{\text{obs}}$  to approximately  $0.18 \text{ gVSS gBOD}^{-1}$ , thereby  
628 favouring the biomass renewing. These results indicated that the removal rate of nitrites did not  
629 show any significant relationship with the increase in salinity ( $p > 0.465$ ), but rather with the SRT.

630

### 631 *3.6 Bacterial community analysis*

632 Due to the promising results on biological performance of the autochthonous halophilic-marine  
633 biomass in both the SBRs also at  $50 \text{ gNaCl L}^{-1}$ , the high-throughput sequencing technology was  
634 applied on such communities to provide a first insight into their microbial diversity. To the best  
635 author's knowledge, although several studies investigated the impact of salinity on microorganisms  
636 in activated sludge processes (He et al. 2017), a few data are available about the bacterial diversity  
637 of halophilic-marine biomass at salinity higher than  $30 \text{ gNaCl L}^{-1}$  (Ji et al. 2018).

638 Both the analyzed microbial communities showed to harbor considerable microbial diversity, with  
639 high species richness (Fig. 5a), despite the high salinity experimented in this study. This can be  
640 explained by the presence of a high number of rare species, as shown by the rank abundance curves  
641 that revealed that these communities were characterized by a strong dominance of a few operational  
642 taxonomic units (OTUs) and a long tail of rare OTUs (Fig. 5b). Abundances of the rare OTUs were  
643 indeed 93.3% and 93% of the total OTUs in AGS-SBR and AS-SBR communities, respectively.  
644 Abundant OTUs were defined as those comprising 1% or more of the community, and rare OTUs  
645 comprised  $< 1\%$  (Campbell et al., 2011).

646 As previously suggested (Besemer, 2016) for other microbial communities, the presence of high  
647 amounts of rare taxa, many of which not actively metabolizing, provides the genetic capability to  
648 respond to changes in environmental conditions.

649 Although the taxon richness resulted to be higher in the AGS-SBR sample (Fig. 5a), the halophilic-  
650 marine biomass showed similar taxon composition in both the SBRs. On phylum level (Fig. 5c),  
651 samples were dominated by OTUs affiliated to Bacteroidetes (60% in AS-SBR and 64% in AGS-  
652 SBR). Proteobacteria were also present at high percentages (31.91 % in AS-SBR and 30.82% in  
653 AGS-SBR), while both the phyla Planctomycetes (1.57% in AS-SBR and 0.30% in AGS-SBR) and  
654 Firmicutes (1.29% in AS-SBR and 1.34% in AGS-SBR) contributed less to the dominant portion of  
655 the communities. Results are in agreement with previous studies revealing Bacteroidetes as one of  
656 the most abundant phylum composing marine microbial communities, due to their important role  
657 played in the organic degradation in such environments (Díez-Vives et al., 2012). Although a direct  
658 comparison with data available in literature is difficult, due to the lack of information on microbial  
659 diversity of halophilic-marine biomass, it should be reasonable compare results obtained here with  
660 the outputs of studies on the effect of salinity on microbial composition in activated processes (He  
661 et al. 2017, Chen et al. 2018, Zhang et al. 2016). Our results seemed to be in agreement with  
662 different studies that revealed the dominance of Proteobacteria, Bacteroidetes and Firmicutes in  
663 activated sludges grown at high salinity conditions (He et al. 2017, Chen et al. 2018, Zhang et al.  
664 2016) and that highlighted the high tolerance to salt stress of Bacteroidetes (Chen et al. 2018).

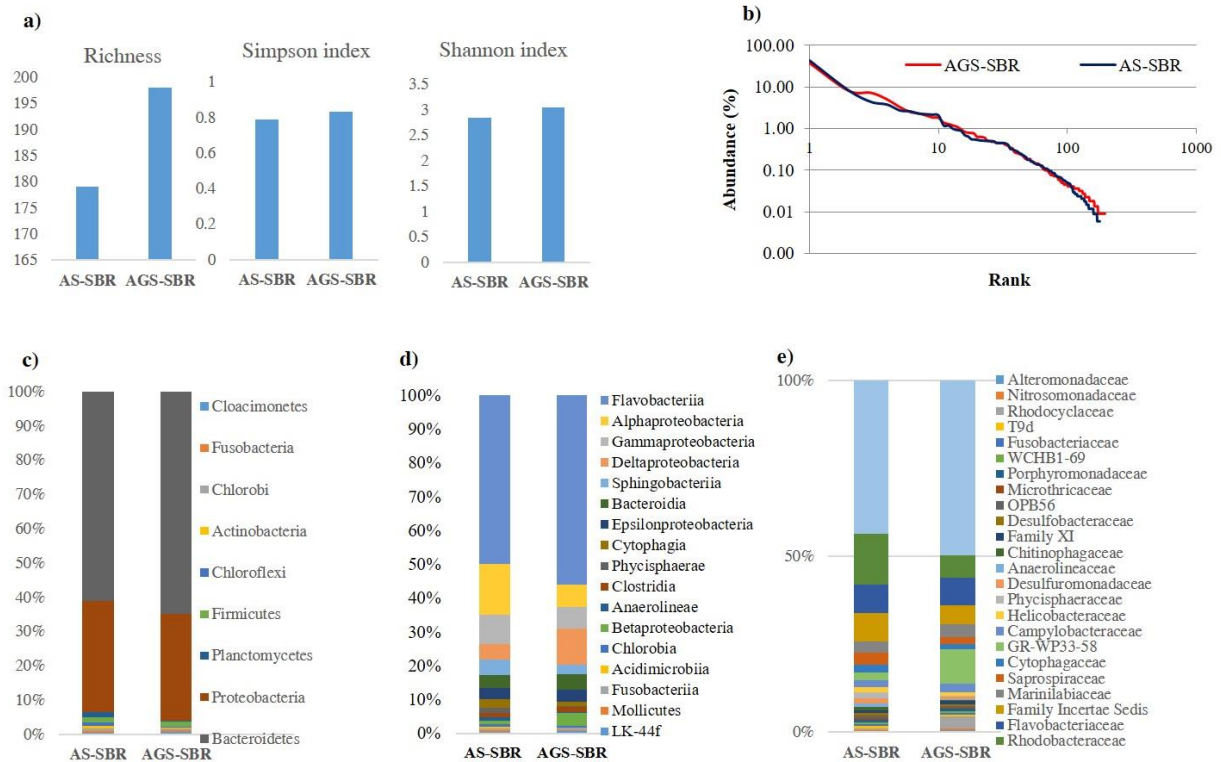
665 From Fig. 5d and Fig. 5e, the community composition on class and family level was further  
666 analyzed. Bacteroidetes were dominated by members of the Flavobacteria (49.20% in AS-SBR and  
667 for 55.37% in AGS-SBR) and included members of the Bacteroidia (3.84% in AS-SBR and 4.53%  
668 in AGS-SBR). Among the Flavobacteria, the family Cryomorphaceae predominated, with the  
669 highest contribution from members of the genus *Owenweeksia* (38 in AS-SBR and 45% in AGS-  
670 SBR). The family Flavobacteriaceae, mainly the genus *Vitellibacter* (7.25% in AS-SBR and 4.40%

671 in AGS-SBR), was also abundant. For the Bacteroidia, *Marinifilum* represented the most abundant  
672 genus (2.09% in AS-SBR and 2.69% in AGS-SBR).

673 Within the Proteobacteria, members of Alpha (14.59% in AS-SBR and 6.72% in AGS-SBR),  
674 Delta-Proteobacteria (4.53 in AS-SBR and 10.76 in AGS-SBR) and Gamma-Proteobacteria (8.53 in  
675 AS-SBR and 6.17 in AGS-SBR) were also prominent. The microbial composition found in the  
676 analyzed samples, can explain the performance of the autochthonous halophilic-marine biomass in  
677 both the SBRs at 50 gNaCl L<sup>-1</sup>. The dominance of Cryomorphaceae in both the samples, indeed,  
678 agrees with the ecology of this family, that comprises primarily marine genera (McBride, 2014a).  
679 Moreover, the dominant genus *Owenweeksia* contains only a single species isolated from sand-  
680 filtered seawater, collected at Port Shelter in Hong Kong (Lau, 2005) and the genera *Vitellibacter*  
681 and *Marinifilum* comprised mainly marine species isolated from seawater (Ruvira et al. 2013,  
682 Thevarajoo et al. 2016, Xu et al. 2016). In addition, the presence of high percentages of members  
683 belonging to Proteobacteria are generally in agreement with studies evaluating the salt tolerance of  
684 microbial communities in activated and granular sludge processes (He et al. 2017, Ji et al. 2018).

685





686 **Fig.5:** Microbial diversity and composition of the halophilic communities grown in the SBRs  
 687 (AGS-SBR and AS-SBR) developed at the highest salinity experimented ( $50 \text{ gNaCl L}^{-1}$ ), obtained  
 688 from NGA data. Microbial diversity, estimated by applying Richness, Simpson and Shannon  
 689 indices (a). Rank–abundance curves of communities for determining population relative  
 690 abundances. Curves are displayed on a log–log scale for clarity (b). Relative abundances (%) of the  
 691 most representative bacterial taxa in microbial communities at phylum (c), class (d) and family (e)  
 692 level. Data are reported as operational taxonomic units (OTUs).  
 693

694  
 695 **4. Discussion**

696 *4.1 Autochthonous or allochthonous biomass?*

697 One of the aim of this study was to compare the performance of the autochthonous biomass with  
 698 that allochthonous acclimated to salinity. The results discussed above indicated that the  
 699 autochthonous halophilic-marine bacteria enabled very high nutrient removal efficiencies compared  
 700 to halotolerant biomasses (He et al., 2017; Zhang et al., 2017). In terms of nutrient removal  
 701 performance, both the SBRs enables more than 95% of the influent organic load ( $2.25 \text{ g COD m}^{-3}\text{d}^{-1}$ )

702 <sup>1</sup>), which resulted higher than that obtained in other studies with acclimated biomass operating at  
703 lower salinity and treating synthetic wastewater (Ji et al., 2018; Ou et al., 2018a; Wang et al., 2014).  
704 While referring to nitrogen removal, complete nitrification was successfully achieved within the  
705 entire range of salinity investigated. In contrast, in previous literature, nitrogen removal is  
706 considered the main concern related to the treatment of saline wastewater. In the majority of the  
707 available studies in the literature, complete nitrification is generally achieved up to 20 gNaCl L<sup>-1</sup>  
708 (Pronk et al., 2014), whereas stable nitritation was achieved up to a salinity of approximately 45  
709 gNaCl L<sup>-1</sup>, although it rapidly collapsed at higher salt concentration (García-Ruiz et al., 2018).  
710 Moreover, in terms of physical structure of the bio-aggregates, it was observed that detrimental  
711 effects on the EPS matrix occurred as a result of long SRT, whereas it was not affected by the  
712 increase in salinity as reported in previous studies with acclimated biomasses (Corsino et al., 2017;  
713 Wang et al., 2016).

714 The results above confirmed that the use of autochthonous-halophilic bacteria represents a valuable  
715 solution for the treatment high-strength carbon and nitrogen saline wastewater. The results also  
716 indicated that both kinetics and performances were significantly higher than those achievable with  
717 acclimated halotolerant microorganisms, even at higher salinity (Lefebvre and Moletta, 2006; Wang  
718 et al., 2017). Results reported in literature suggest that although the acclimatization of conventional  
719 activated sludge to the salinity is possible (Lefebvre and Moletta, 2006; van den Akker et al., 2015;  
720 Wang et al., 2015), the achievement of high ammonium oxidation rates and nitrogen removal  
721 efficiencies is limited within a range of salinity between 5 gNaCl L<sup>-1</sup> and 33 gNaCl L<sup>-1</sup> (Pronk et al.,  
722 2014; Wang et al., 2017). Moreover, the autochthonous biomass had a better biodiversity compared  
723 to the acclimated biomass as proven by the considerable microbial diversity that gained a higher  
724 nutrient removal performances and process stability at high salinity levels.

725 It is worth mentioning that a comparison between the results above with others referred to the  
726 autochthonous-halophilic biomass under similar operating conditions was not carried out because of  
727 the lack of knowledge in the literature. Besides, the achieved results suggested that halophilic

728 biomass could tolerate higher salinity levels than those tested in this study. However, it has to be  
729 mentioned that under higher salinity levels several technical drawbacks could occur, like salt  
730 deposits on equipment and devices, as well as scaling on the air diffuser that create management  
731 difficulties independently on the effects of the salinity on the bacterial metabolism.

732 The result discussed above demonstrated that the start-up of a plant designed for the treatment of a  
733 saline wastewater with an inoculum of autochthonous biomass is more appropriated than using  
734 allochthonous bacteria. Indeed, the cultivation of the autochthonous biomass offers benefits in terms  
735 of higher metabolic kinetics, higher microbial diversity, stable process operation, thereby enabling  
736 an effluent of superior quality, while saving energy and footprint. Therefore, both from a  
737 management and process point of view, the system's start-up without any inoculum, thus allowing  
738 developing the autochthonous biomass, represent a valuable operating strategy to achieve highly  
739 performing systems.

740

#### 741 *4.2 Granular or activated sludge?*

742 Overall, biological performances were comparable in both the activated and the granular sludge  
743 reactors, thereby indicating that, when a stepwise increase strategy of the salinity is performed, the  
744 granulation process did not provide significant improvements in the nutrient removal processes.  
745 Previous studies demonstrated that the aerobic granulation of halophilic sludge offers an advantage  
746 in case of drastic salinity fluctuations (Corsino et al., 2018). Indeed, because of the bigger and  
747 denser structure the aerobic granules are able to withstand drastic and moderate salinity fluctuations  
748 in the short and long-term better than activated sludge. Nonetheless, if a stepwise strategy of  
749 salinity increases is performed, the halophilic activated sludge shows a similar response to salinity  
750 increases compared to halophilic granular sludge. The bacterial community analysis did not  
751 highlight significant differences between the AGS-SBR and AS-SBR. Indeed, although the taxon  
752 richness resulted to be higher in the AGS-SBR sample, the halophilic-marine biomass showed a  
753 very similar taxon composition in both the SBRs.

754 Biological performances resulted mostly affected by the SRT and by the decreasing solubility of the  
755 oxygen due to the salinity in both the systems. Indeed, the oxygen transfer and diffusion processes,  
756 as well as the biomass ageing significantly affected both the carbon and the nitrogen removal  
757 kinetics and performances more than salinity. This was more noticeable in the AGS-SBR because  
758 of the higher size and density of the microbial aggregates that represented an additional barrier to  
759 the oxygen diffusion and favoured the buildup of inert material.

760 Nevertheless, although the kinetic and the biological performances were comparable within the  
761 entire range of salinity investigated in this study, it is worth mentioning that, because of the higher  
762 biomass retention capacity, AGS systems could be able to enable almost 50% of volume saving.

763

## 764 **5. Conclusions**

765 Nutrient removal performances and kinetics of autochthonous marine bacteria in forms of activated  
766 and granular sludge were assessed at different salinity levels, ranging from 30 gNaCl L<sup>-1</sup> to 50  
767 gNaCl L<sup>-1</sup> in two SBRs. The achieved results demonstrated that the cultivation of the autochthonous  
768 biomass offers benefits in terms of higher metabolic kinetics, higher microbial diversity and stable  
769 process operation than allochthonous acclimated biomass, thereby enabling an effluent of superior  
770 quality. At the maximum salinity level tested, the microbial community was dominated in both the  
771 systems by marine species belonged to the genera *Owenweeksia* (Cryomorphaceae), *Vitellibacter*  
772 (Flavobacteriaceae) and *Marinifilum* (Bacteroidia). Both the SBRs provided a high-quality effluent,  
773 enabling performances approximately of 98% and 90% in terms of carbon removal and nitrification  
774 efficiency, respectively. Denitrification process was limited independently of salinity, resulting in TN  
775 removal efficiency lower than 70%. Nevertheless, the biomass activity and performances slightly  
776 decreased as a result of a long SRT (27 days) because of salt accumulation within the activated  
777 sludge flocs and granules. Although the high salinity, AUR and NUR of approximately 3.60  
778 mgNH<sub>4</sub>-N gVSS<sup>-1</sup>h<sup>-1</sup> and 10.0 mgNO<sub>2</sub>-N gVSS<sup>-1</sup>h<sup>-1</sup>, respectively, indicated a high activity of  
779 nitrifying and denitrifying bacteria. The obtained results also indicated that a lower SRT (14 days),

780 favoured the discharge of the granules and flocs with higher inert content, thereby enhancing the  
781 biomass renewing and a high metabolic activity. The operating strategy of stepwise increasing the  
782 salinity and decreasing the SRT is crucial for a dual proposal when treating saline wastewater: first  
783 to avoid an excessive buildup of salt within the biomass aggregates and second to avoid their  
784 physical deconstruction. Indeed, both the strategies enabled to achieve sludge with good physical  
785 properties, because of the decrease in the LB-EPS fraction. Lastly, if a stepwise strategy of salinity  
786 increases is performed, the halophilic activated sludge shows a similar response to salinity increases  
787 compared to halophilic granular sludge.

788

### 789 **Acknowledgements**

790 The Authors have the very sad duty to inform that our Coauthor, Dr. Valter Tandoi, passed away  
791 before the manuscript's submission. The Authors would like to warmly thank Dr. Tandoi for his  
792 extremely valuable contribution for this paper.

793

### 794 **References**

795 Albertsen, M., Karst, S.M., Ziegler, A.S., Kirkegaard, R.H., Nielsen, P.H., 2015. Back to basics -

796 The influence of DNA extraction and primer choice on phylogenetic analysis of activated  
797 sludge communities. *PLoS One* 10. doi:10.1371/journal.pone.0132783

798 APHA, 2005. *Standard Methods for the Examination of Water & Wastewater*, American Public  
799 Health Association.

800 Bernat, K., Wojnowska-Baryła, I., Dobrzyńska, A., 2008. Denitrification with endogenous carbon  
801 source at low C/N and its effect on P(3HB) accumulation. *Bioresour. Technol.* 99, 2410–2418.  
802 doi:10.1016/j.biortech.2007.05.008

803 Besemer K., 2016. Europe PMC Funders Group Biodiversity, community structure and function of  
804 biofilms in stream ecosystems. *Res Microbiol.* 166(10), 774–781.

805 doi:10.1016/j.resmic.2015.05.006

806 Bolger, A.M., Lohse, M., Usadel, B., 2014. Trimmomatic: A flexible trimmer for Illumina sequence  
807 data. *Bioinformatics* 30, 2114–2120. doi:10.1093/bioinformatics/btu170

808 Campbell, B.J., Yu, L., Heidelberg, J.F., Kirchman, D.L., 2011. Activity of abundant and rare  
809 bacteria in a coastal ocean. *Proc Natl Acad Sci USA*. 108:12776–12781.  
810 doi:10.1073/pnas.1101405108

811 Campo, R., Fabio Corsino, S., Torregrossa, M., Di Bella, G., 2018. The role of extracellular  
812 polymeric substances on aerobic granulation with stepwise increase of salinity. *Sep. Purif.*  
813 *Technol.* 195, 12–20. doi:https://doi.org/10.1016/j.seppur.2017.11.074

814 Capodici, M., Corsino, S.F., Torregrossa, M., Viviani, G., 2018. Shortcut nitrification-  
815 denitrification by means of autochthonous halophilic biomass in an SBR treating fish-canning  
816 wastewater. *J. Environ. Manage.* 208, 142–148. doi:10.1016/j.jenvman.2017.11.055

817 Caporaso, J.G., Kuczynski, J., Stombaugh, J., Bittinger, K., Bushman, F.D., Costello, E.K., Fierer,  
818 N., Peña, A.G., Goodrich, J.K., Gordon, J.I., Huttley, G. a, Kelley, S.T., Knights, D., Koenig,  
819 J.E., Ley, R.E., Lozupone, C. a, Mcdonald, D., Muegge, B.D., Pirrung, M., Reeder, J.,  
820 Sevinsky, J.R., Turnbaugh, P.J., Walters, W. a, Widmann, J., Yatsunenko, T., Zaneveld, J.,  
821 Knight, R., 2010. correspondence QIIME allows analysis of high- throughput community  
822 sequencing data Intensity normalization improves color calling in SOLiD sequencing. *Nat.*  
823 *Publ. Gr.* 7, 335–336. doi:10.1038/nmeth0510-335

824 Chen, Y., He, H., Liu, H., Li, H., Zeng, G., Xia, X., Yang, C., 2018. Effect of salinity on removal  
825 performance and activated sludge characteristics in sequencing batch reactors. *Bioresour.*  
826 *Technol.* 249, 890–899. doi:10.1016/j.biortech.2017.10.092

827 Ching, Y.C., Redzwan, G., 2017. Biological Treatment of Fish Processing Saline Wastewater for

828 Reuse as Liquid Fertilizer. 9 (7), 1062-1088. doi:10.3390/su9071062

829 Chowdhury, P., Viraraghavan, T., Srinivasan, a., 2010. Biological treatment processes for fish  
830 processing wastewater - A review. *Bioresour. Technol.* 101, 439–449.  
831 doi:10.1016/j.biortech.2009.08.065

832 Corsino, S.F., Capodici, M., Morici, C., Torregrossa, M., Viviani, G., 2016. Simultaneous  
833 nitritation–denitritation for the treatment of high-strength nitrogen in hypersaline wastewater  
834 by aerobic granular sludge. *Water Res.* 88, 329–336. doi:10.1016/j.watres.2015.10.041

835 Corsino, S.F., Capodici, M., Torregrossa, M., Viviani, G., 2018. A comprehensive comparison  
836 between halophilic granular and flocculent sludge in withstanding short and long-term salinity  
837 fluctuations. *J. Water Process Eng.* 22, 265–275. doi:10.1016/j.jwpe.2018.02.013

838 Corsino, S.F., Capodici, M., Torregrossa, M., Viviani, G., 2017. Physical properties and  
839 Extracellular Polymeric Substances pattern of aerobic granular sludge treating hypersaline  
840 wastewater. *Bioresour. Technol.* 229, 152–159.  
841 doi:http://doi.org/10.1016/j.biortech.2017.01.024

842 Cui, Y.W., Zhang, H.Y., Ding, J.R., Peng, Y.Z., 2016. The effects of salinity on nitrification using  
843 halophilic nitrifiers in a Sequencing Batch Reactor treating hypersaline wastewater. *Sci. Rep.*  
844 6, 24825. doi:10.1038/srep24825

845 Decho, A.W., 2013. The EPS matrix as an adaptive bastion for biofilms: Introduction to special  
846 issue. *Int. J. Mol. Sci.* 14, 23297–23300. doi:10.3390/ijms141223297

847 Decho, A.W., Gutierrez, T., 2017. Microbial extracellular polymeric substances (EPSs) in ocean  
848 systems. *Front. Microbiol.* 8. doi:10.3389/fmicb.2017.00922

849 Díez-Vives, C., Gasol, J.M., Acinas, S.G., 2012. Evaluation of marine bacteroidetes-specific  
850 primers for microbial diversity and dynamics studies. *Microb Ecol.* 64(4), 1047-55. doi:

851 10.1007/s00248-012-0087

852 DuBois, M., Gilles, K. a., Hamilton, J.K., Rebers, P. a., Smith, F., 1956. Colorimetric method for  
853 determination of sugars and related substances. *Anal. Chem.* 28, 350–356.  
854 doi:10.1021/ac60111a017

855 Edgar, R.C., 2013. UPARSE: Highly accurate OTU sequences from microbial amplicon reads. *Nat.*  
856 *Methods* 10, 996–998. doi:10.1038/nmeth.2604

857 Fan, J., Zhang, J., Zhang, C., Ren, L., Shi, Q., 2011. Adsorption of 2,4,6-trichlorophenol from  
858 aqueous solution onto activated carbon derived from loosestrife. *Desalination* 267, 139–146.  
859 doi:10.1016/j.desal.2010.09.016

860 Figueroa, M., Mosquera-Corral, A., Campos, J.L., Méndez, R., 2008. Treatment of saline  
861 wastewater in SBR aerobic granular reactors. *Water Sci. Technol.* 58, 479.  
862 doi:10.2166/wst.2008.406

863 García-Ruiz, M.J., Castellano-Hinojosa, A., González-López, J., Osorio, F., 2018. Effects of  
864 salinity on the nitrogen removal efficiency and bacterial community structure in fixed-bed  
865 biofilm CANON bioreactors. *Chem. Eng. J.* 347, 156–164. doi:10.1016/j.cej.2018.04.067

866 Giesen, A., de Bruin, L.M.M., Niermans, R.P., ven der Roest, H.F., 2013. Advancements in the  
867 application of aerobic granular biomass technology for sustainable treatment of wastewater.  
868 *Water Pract. Technol.* 8, 47–54.

869 Gomes, M.B., Gonzales-Limache, E.E., Sousa, S.T.P., Dellagnezze, B.M., Sartoratto, A., Silva,  
870 L.C.F., Gieg, L.M., Valoni, E., Souza, R.S., Torres, A.P.R., Sousa, M.P., De Paula, S.O., Silva,  
871 C.C., Oliveira, V.M., 2018. Exploring the potential of halophilic bacteria from oil terminal  
872 environments for biosurfactant production and hydrocarbon degradation under high-salinity  
873 conditions. *Int. Biodeterior. Biodegradation* 126, 231–242. doi:10.1016/j.ibiod.2016.08.014



- 874 Guo, G., He, F., Tian, F., Huang, Y., Wang, H., 2016. Effect of salt contents on enzymatic activities  
875 and halophilic microbial community structure during phenanthrene degradation. *Int.*  
876 *Biodeterior. Biodegrad.* 110, 8–15. doi:10.1016/j.ibiod.2016.02.007
- 877 Hill, M., 1973. Diversity and evenness: a unifying notation and its consequences. *Ecology* 54, 427–  
878 432. doi:10.2307/1934352. doi:10.2307/1934352
- 879 He, H., Chen, Y., Li, X., Cheng, Y., Yang, C., Zeng, G., 2017. Influence of salinity on  
880 microorganisms in activated sludge processes: A review. *Int. Biodeterior. Biodegradation* 119,  
881 520–527. doi:10.1016/j.ibiod.2016.10.007
- 882 Ismail, S.B., de La Parra, C.J., Temmink, H., van Lier, J.B., 2010. Extracellular polymeric  
883 substances (EPS) in upflow anaerobic sludge blanket (UASB) reactors operated under high  
884 salinity conditions. *Water Res.* 44, 1909–1917. doi:10.1016/j.watres.2009.11.039
- 885 Jemli, M., Karray, F., Feki, F., Loukil, S., Mhiri, N., Aloui, F., Sayadi, S., 2015. Biological  
886 treatment of fish processing wastewater: A case study from Sfax City (Southeastern Tunisia).  
887 *J. Environ. Sci. (China)* 30, 102–112. doi:10.1016/j.jes.2014.11.002
- 888 Ji, J., Peng, Y., Wang, B., Mai, W., Li, X., Zhang, Q., Wang, S., 2018. Effects of salinity build-up  
889 on the performance and microbial community of partial-denitrification granular sludge with  
890 high nitrite accumulation. *Chemosphere* 209, 53–60. doi:10.1016/j.chemosphere.2018.05.193
- 891 Lang, K.S., Lang, P.A., Bauer, C., Durantón, C., Wieder, T., Huber, S.M., Lang, F., 2005.  
892 Mechanisms of suicidal erythrocyte death. *Cell. Physiol. Biochem.* doi:10.1159/000086406
- 893 Lau, K. W. K., 2005. *Owenweeksia hongkongensis* gen. nov., sp. nov., a novel marine bacterium of  
894 the phylum 'Bacteroidetes'. *International Journal of systematic and evolutionary microbiology*  
895 55 (3), 1051-1057. doi.org:10.1099/ijs.0.63155-0
- 896 Le-Clech, P., Chen, V., Fane, T. a G., 2006. Fouling in membrane bioreactors used in wastewater

897 treatment. *J. Memb. Sci.* 284, 17–53. doi:10.1016/j.memsci.2006.08.019

898 Lefebvre, O., Moletta, R., 2006. Treatment of organic pollution in industrial saline wastewater: A  
899 literature review. *Water Res.* 40, 3671–3682. doi:10.1016/j.watres.2006.08.027

900 Lowry, O.H., Rosebrough, N.J., Farr, L., Randall, R., 1951. Protein measurement with the folin  
901 phenol reagent. *J. Biol. Chem.* 193, 265–275. doi:10.1016/0304-3894(92)87011-4

902 Magoč, T., Salzberg, S.L., 2011. FLASH: Fast length adjustment of short reads to improve genome  
903 assemblies. *Bioinformatics* 27, 2957–2963. doi:10.1093/bioinformatics/btr507

904 Mannina, G., Cosenza, A., Di Trapani, D., Capodici, M., Viviani, G., 2016. Membrane bioreactors  
905 for treatment of saline wastewater contaminated by hydrocarbons (diesel fuel): An  
906 experimental pilot plant case study. *Chem. Eng. J.* 291, 269–278.  
907 doi:10.1016/j.cej.2016.01.107

908 McBride, M.J., 2014a. The Family Flavobacteriaceae. In: Rosenberg E., DeLong E.F., Lory S.,  
909 Stackebrandt E., Thompson F. (eds). *The Prokaryotes*. Springer, Berlin, Heidelberg. ISBN  
910 978-3-642-38954-2

911 McBride, M.J., 2014b. The Family Cryptomonaceae. In: Rosenberg E., DeLong E.F., Lory S.,  
912 Stackebrandt E., Thompson F. (eds) *The Prokaryotes*. Springer, Berlin, Heidelberg. ISBN 978-  
913 3-642-38954-2

914 McIlroy, S.J., Saunders, A.M., Albertsen, M., Nierychlo, M., McIlroy, B., Hansen, A.A., Karst,  
915 S.M., Nielsen, J.L., Nielsen, P.H., 2015. MiDAS: The field guide to the microbes of activated  
916 sludge. *Database* 2015. doi:10.1093/database/bav062

917 Metcalf, Eddy, 2015. *Wastewater Engineering Treatment and Resource Recovery*. 5th ed. McGraw-  
918 Hill.

919 Muthukumar, S., Baskaran, K., 2013. Organic and nutrient reduction in a fish processing facility -

920 A case study. *Int. Biodeterior. Biodegrad.* 85, 563–570. doi:10.1016/j.ibiod.2013.03.023

921 Oren, A., 2010. Industrial and environmental applications of halophilic microorganisms. *Environ.*  
922 *Technol.* 31(8-9), 825-34. doi:10.1080/09593330903370026

923 Ou, D., Li, H., Li, W., Wu, X., Wang, Y., Liu, Y., 2018a. Salt-tolerance aerobic granular sludge:  
924 Formation and microbial community characteristics. *Bioresour. Technol.* 249, 132–138.  
925 doi:10.1016/j.biortech.2017.07.154

926 Ou, D., Li, W., Li, H., Wu, X., Li, C., Zhuge, Y., Liu, Y., 2018b. Enhancement of the removal and  
927 settling performance for aerobic granular sludge under hypersaline stress. *Chemosphere* 212,  
928 400–407. doi:10.1016/j.chemosphere.2018.08.096

929 Pronk, M., Bassin, J.P., de Kreuk, M.K., Kleerebezem, R., van Loosdrecht, M.C.M., 2014.  
930 Evaluating the main and side effects of high salinity on aerobic granular sludge. *Appl.*  
931 *Microbiol. Biotechnol.* 98, 1339–48. doi:10.1007/s00253-013-4912-z

932 Ramos, C., Suárez-Ojeda, M.E., Carrera, J., 2015. Long-term impact of salinity on the performance  
933 and microbial population of an aerobic granular reactor treating a high-strength aromatic  
934 wastewater. *Bioresour. Technol.* 198, 844–851. doi:10.1016/j.biortech.2015.09.084

935 Ruvira, M.A., Lucena, T., Pujalte, M.J., Arahal, D.R., Macián, M.C., 2009. *Marinifilum flexuosum*  
936 *sp. nov.*, a new Bacteroidetes isolated from coastal Mediterranean Sea water and emended  
937 description of the genus *Marinifilum* Na et al., 2009. *Syst Appl Microbiol.* 36(3), 155-159. doi:  
938 10.1016/j.syapm.2012.12.003.

939 Thevarajoo, S., Selvaratnam, C., Goh, K.M., Hong, K.W., Chan, X.Y., Chan, K.G., Chong, C.S.,  
940 2016. *Vitellibacter aquimaris sp. nov.*, a marine bacterium isolated from seawater. *Int J Syst*  
941 *Evol Microbiol.* 66(9), 3662-3668. doi: 10.1099/ijsem.0.001248.

942 Val del Río, A., Figueroa, M., Arrojo, B., Mosquera-Corral, A., Campos, J.L., García-Torriello, G.,

943 Méndez, R., 2012. Aerobic granular SBR systems applied to the treatment of industrial  
944 effluents. *J. Environ. Manage.* 95, S88–S92. doi:10.1016/j.jenvman.2011.03.019

945 van den Akker, B., Reid, K., Middlemiss, K., Krampe, J., 2015. Evaluation of granular sludge for  
946 secondary treatment of saline municipal sewage. *J. Environ. Manage.* 157, 139–145.  
947 doi:10.1016/j.jenvman.2015.04.027

948 Wang, Q., Garrity, G.M., Tiedje, J.M., Cole, J.R., 2007. Naïve Bayesian classifier for rapid  
949 assignment of rRNA sequences into the new bacterial taxonomy. *Appl. Environ. Microbiol.*  
950 73, 5261–5267. doi:10.1128/AEM.00062-07

951 Wang, X., Yang, T., Lin, B., Tang, Y., 2017. Effects of salinity on the performance, microbial  
952 community, and functional proteins in an aerobic granular sludge system, ECSN.  
953 doi:10.1016/j.chemosphere.2017.06.047

954 Wang, Z., Gao, M., She, Z., Wang, S., Jin, C., Zhao, Y., 2015. Effects of salinity on performance ,  
955 extracellular polymeric substances and microbial community of an aerobic granular  
956 sequencing batch reactor. *Sep. Purif. Technol.* 144, 223–231.  
957 doi:10.1016/j.seppur.2015.02.042

958 Wang, Z., Gao, M., Wei, J., Ma, K., Pei, J., Zhang, J., Zhou, Y., Yang, Y., Yu, S., 2016. Long-term  
959 effects of salinity on extracellular polymeric substances, microbial activity and microbial  
960 community from biofilm and suspended sludge in an anoxic-aerobic sequencing batch biofilm  
961 reactor. *J. Taiwan Inst. Chem. Eng.* 68, 275–280. doi:10.1016/j.jtice.2016.09.005

962 Wang, Z., van Loosdrecht, M.C.M., Saikaly, P.E., 2017. Gradual adaptation to salt and dissolved  
963 oxygen: Strategies to minimize adverse effect of salinity on aerobic granular sludge. *Water*  
964 *Res.* 124, 702–712. doi:10.1016/j.watres.2017.08.026

965 Ward, D. V., Gevers, D., Giannoukos, G., Earl, A.M., Methé, B.A., Sodergren, E., Feldgarden, M.,

966 Ciulla, D.M., Tabbaa, D., Arze, C., Appelbaum, E., Aird, L., Anderson, S., Ayvaz, T., Belter,  
967 E., Bihan, M., Bloom, T., Crabtree, J., Courtney, L., Carmichael, L., Dooling, D., Erlich, R.L.,  
968 Farmer, C., Fulton, L., Fulton, R., Gao, H., Gill, J.A., Haas, B.J., Hemphill, L., Hall, O.,  
969 Hamilton, S.G., Hepburn, T.A., Lennon, N.J., Joshi, V., Kells, C., Kovar, C.L., Kalra, D., Li,  
970 K., Lewis, L., Leonard, S., Muzny, D.M., Mardis, E., Mihindikulasuriya, K., Magrini, V.,  
971 O’Laughlin, M., Pohl, C., Qin, X., Ross, K., Ross, M.C., Rogers, Y.H.A., Singh, N., Shang,  
972 Y., Wilczek-Boney, K., Wortman, J.R., Worley, K.C., Youmans, B.P., Yooseph, S., Zhou, Y.,  
973 Schloss, P.D., Wilson, R., Gibbs, R.A., Nelson, K.E., Weinstock, G., DeSantis, T.Z.,  
974 Petrosino, J.F., Highlander, S.K., Birren, B.W., 2012. Evaluation of 16s rDNA-based  
975 community profiling for human microbiome research. PLoS One 7.  
976 doi:10.1371/journal.pone.0039315

977 Winkler, M.K.H., Bassin, J.P., Kleerebezem, R., Sorokin, D.Y., Van Loosdrecht, M.C.M., 2012.  
978 Unravelling the reasons for disproportion in the ratio of AOB and NOB in aerobic granular  
979 sludge. Appl. Microbiol. Biotechnol. 94, 1657–1666. doi:10.1007/s00253-012-4126-9

980 Wu, G., Guan, Y., Zhan, X., 2008. Effect of salinity on the activity, settling and microbial  
981 community of activated sludge in sequencing batch reactors treating synthetic saline  
982 wastewater. Water Sci. Technol. 58, 351–358. doi:10.2166/wst.2008.675

983 Xingang Wang, Bing Lin, Yubin Tang, Chen, H., 2014. Effects of high salinity on the removal of  
984 pollutants in wastewater by aerobic granular sludge. Adv. Mater. Res. 955–959, 339–342.  
985 doi:10.4028/www.scientific.net/AMR.955-959.339

986 Zhen-Xing, X., Xin, M., Heng-Xi, Z., Guan-Jun, C., Zong-Jun, Du., 2016. *Marinifilum*  
987 *albidiflavum* sp. nov., isolated from coastal sediment. International Journal of Systematic and  
988 Evolutionary Microbiology 66, 4589–4593. doi:10.1099/ijsem.0.001395

989 Zannotti, M., Giovannetti, R., 2015. Kinetic evidence for the effect of salts on the oxygen solubility

990 using laboratory prototype aeration system. *J. Mol. Liq.* 211, 656–666.

991 doi:10.1016/j.molliq.2015.07.063

992 Zhang, Y., Jiang, W.-L., Xu, R.-X., Wang, G.-X., Xie, B., 2017. Effect of short-term salinity shock  
993 on unacclimated activated sludge with pressurized aeration in a sequencing batch reactor. *Sep.*  
994 *Purif. Technol.* 178, 200–206.

995 Zhao, L., She, Z., Jin, C., Yang, S., Guo, L., Zhao, Y., Gao, M., 2016. Characteristics of  
996 extracellular polymeric substances from sludge and biofilm in a simultaneous nitrification and  
997 denitrification system under high salinity stress. *Bioprocess Biosyst. Eng.* 39, 1375–1389.  
998 doi:10.1007/s00449-016-1613-x

999 Zhao, Y., Park, H.-D., Park, J.-H., Zhang, F., Chen, C., Li, X., Zhao, D., Zhao, F., 2016. Effect of  
1000 different salinity adaptation on the performance and microbial community in a sequencing  
1001 batch reactor. *Bioresour. Technol.* 216, 808–816. doi:10.1016/j.biortech.2016.06.032

1002 Zhuang, X., Han, Z., Bai, Z., Zhuang, G., Shim, H., 2010. Progress in decontamination by  
1003 halophilic microorganisms in saline wastewater and soil. *Environ. Pollut.* 158(5), 1119-1126.  
1004 doi:10.1016/j.envpol.2010.01.007

1005

1006

1007

1008

1009

1010

1011

1012

1013

1014

1015 **Figure caption**

1016 **Fig.1:** Trends of the specific EPS content and percentage of loosely-bound EPS in the activated  
1017 sludge (AS) and granular sludge (AGS) reactors.

1018 **Fig.2:** Influent and effluent concentrations for BOD (a) and COD (c) and the removal efficiencies  
1019 (b,d) during the eleven experimental phases.

1020 **Fig.3:** Influent and effluent concentrations of the ammonium and nitrite in the AGS-SBR and AS-  
1021 SBR (a) and nitrification efficiency (b) at different salinity; influent and effluent concentrations of TN  
1022 (c) and removal efficiencies (d).

1023 **Fig. 4:** Values of the ammonium utilization rate (a) and the nitrite utilization rate (b) in each Phase  
1024 of the experiment.

1025 **Fig.5:** Microbial diversity and composition of the halophilic communities grown in the SBRs  
1026 (AGS-SBR and AS-SBR) developed at the highest salinity experimented (50 gNaCl L<sup>-1</sup>), obtained  
1027 from NGA data. Microbial diversity, estimated by applying Richness, Simpson and Shannon  
1028 indices (a). Rank–abundance curves of communities for determining population relative  
1029 abundances. Curves are displayed on a log–log scale for clarity (b). Relative abundances (%) of the  
1030 most representative bacterial taxa in microbial communities at phylum (c), class (d) and family (e)  
1031 level. Data are reported as operational taxonomic units (OTUs).

1032

1033 **Fig.S1:** Trends of ammonium and nitrite during a typical SBR cycle in the AGS and AS systems  
1034 (Phase 1)

1035

1036 **Table caption**

1037 **Tab. 1:** Operating conditions for AGS-SBR and AS-SBR during the experimental phases.

1038 **Tab. 2:** Physical properties of granular and activated sludge at different salinity.

1039